AGU PUBLICATIONS

Earth and Space Science

Supporting Information for

Australasian Tektite (AAT) Suborbital Transport Assessment

T. H. S. Harris[1]

[1]GE Astro Space Div., Lockheed Martin, Boeing Helicopter, retired

Contents of this file

Additional Supporting Information (Files uploaded separately)

Captions for Tables S1 to Sx (if larger than 1 page, upload as separate file)
Captions for Movies S1 to Sx
Captions for Audio S1 to Sx

Introduction

[Type or paste your text here. The introduction gives a brief overview of the supporting information. You should include information about as many of the following as possible (when appropriate):

- a general overview of the kind of data files;
- a general description of processing steps used;
- any known imperfections or anomalies in the data.]

INTRODUCTION

Troubles With S. E. Asia as the AAT Source Region

Presented inverse suborbital solutions trend across Earth's surface in various patterns, both to Huai Om, Thailand as a tektite fall point and also from the surrounding regional setting of S. E. Asia (Indochina). Tada et al. (2022) describes an ejecta deposit of the Australasian tektite (AAT) event, containing a well-defined tektite-bearing stratigraphic sequence at Huai Om, making this site an important example of legacy consensus that assumes a S. E. Asia AAT event source region. It is site is also important for the proposed AAT source region of this work, as described in Section 4 of the main manuscript. Several sets of suborbital analysis output are presented, each for its own comparative value within the overall AAT source mystery.

Tektite Ablation Regime Assessment and Decoding

Supplement 1 (S1) presents a single plot of *Helix* results, indicating a general lack of suborbital access availability to the Central Indian Ocean (CIO) ablated button tektite detailed in Glass, Chapman, Prasad (1996) through the defined ablation regime of that specimen, the shaded region of the diagram. The ablation regimes, derived from 1960s NASA tektite ablation research per Chapman, Larson (1963) and Chapman (1964) represent windows of possible atmospheric reentry conditions to generate observed ablation of the tektite(s) they describe. The ablation regime 'windows' are derived from a single line that follows a given constant-ablation curve from lower left to upper right in the diagram.

The ablation condition 'windows' are typically further bounded at their upper and lower ends by dynamic pressure curves running in sub-normal directions relative to the constant-ablation curves. The ablation regime windows may be thought of as ridgelines, where confidence is highest along the ridge, away from its endpoints. From those high-confidence ridgelines, confidence decreases along the sides (flanking margins) and at each end of the ridgeline. The ramp-down effects are based on errors of measurement and also derived from uncertainties that arise from basic unknowns of the tektite ablation paradigm.

The 1960s NASA references are illuminating in terms of seemingly conflicting indications uncovered during that tektite ablation research. Some tektites are naturally ablated literally beyond Earth-escape speed, while an '*undisturbed* atmospheric column' was always assumed in the testing and subsequent derivations. This assumption is apparently at the root of the associated uncertainties, as indicated in the presented findings of this work. The suggested scale of the AAT event is very large to account for these observations, as explained in the manuscript.

The iso-ablation and isobaric curves of NASA's 1960s tektite ablation research is reproduced as an extension of the supplied version of the *Helix* suborbital solver, with the root solver mechanics verified by Walter Alvarez against his own personal in-kind solver for Harris (2022). The reproduction is graphically-based, while adhering to the plots of the 1960s work more consistency than common minor variations between those individual publications. The 1960s work used hand-drawn versus computer-generated plots, with French-curve drafting aids as the primary graphical tool of the day for science and engineering plots.

While hand-drawn plots suggest a general degree of imprecision within reporting of tektite ablation data of 1960s NASA research, important mitigating factors must be considered. First, graphical presentation inconsistencies were far smaller than the unknowns of the tektite ablation itself, again, most likely due to the 'undisturbed atmosphere' assumption. Second and more importantly, the ablation process represents a continuum, both in the physical motion of the ablating tektites (momentum continuum) and in the actual mass loss through melt (mainly) and vaporization (secondarily) that define this ablation regime near Earth's escape speed of ~11.175 km/s (i.e., heat and mass flow continuum).

Because of these various degrees of uncertainty, the ridgeline analogy for ablation windows with ramping-down of flanking slopes ridge-end features applies. The ramp-down concept complicates efforts to place weighting on one set of *Helix* solution curves vs. another as viewed in the ablation diagram paradigm. Ramping and ridgeline definition are required for quantitative differences between one or another ***A***-to-***B*** suborbital (*Helix*) solution set for a given ablation regime. The provided *Helix* spreadsheet bears relict coding for such an attempt. Ultimately, however, the resulting quantitative differences are only as good as the ramp-down definitions at all margins of every ridgeline, thus compromising any attempt from the start. For this reason, a more qualitative approach must be applied.

Supplement 4 (S4) *Helix* results are offered for the implied N. American AAT source region of this work ('midWest swath' and/or Lake Huron, essentially 'suborbitally synonymous') as well as for the legacy consensus S. E. Asia region, typically using Huai Om, Thailand as a defined point on the globe.

While comparing the two sets of suborbital solution family plots of *Helix* results projected within the ablation regime diagrams, we must think of 'ridge-margin incursions' (never more than slightly or part way from ridge-base toward ridge-crest) versus 'ridge-crossing' or 'ridge-crest-loitering' to assess increasing degrees of ablation imprint-matching likelihood, respectively. The ridgeline analogy is a subjective or qualitative assessment process, as an additional tool within an overall critique of the tektite ablation paradigm. The ridgeline analogy is, in fact, closely comparable with geochemistry applied to tektite compositional characterization, an assessment paradigm where finer details of exact measurement may not be as individually meaningful as bigger-picture trends or features of the continuum. Both concepts involve trend identification within larger continuum paradigms, while each may be argued ad-nauseam at minutia-scale for little net gain. The key to both concepts are the big-picture trends within. For the ablation assessment, 'ridgeline traverse' is a valuable concept because it may be applied regardless of one's technical or academic specialty. This is most important during the interdisciplinary exploits of planetary impact research, per Alvarez (1990).

'Ridgeline traverse' assessment provides a baseline reference framework while considering ***A***-to-***B*** suborbital accessibility as constrained by NASA tektite ablation regime data. The problematic portion of such considerations is the degree of ramping or 'blurring' of the ablation signature. This is an important concept that separates more- vs. less-useful ablation signatures. Different ablation family trends may have wide ramp-down margins vs. narrow, concise ridges, making the latter more useful for assessment than the former. This is where the concept of 'primary' versus 'secondary' ablation data becomes useful.

‘Primary’ Ablation Data is Preferred for Best Assessment

The most narrowly-defined or highest-confidence tektite cases are termed ‘primary’ in this work for reasons explained above. In the NASA research of the 1960s, two highest-confidence ‘primary’ cases are explained in Section 1 and subsequently within the main manuscript. These favored ‘primary’ ablation cases, when considered together, indicate a N. American source region by their intersection over continental landmass to account for the Upper Continental Crust (UCC) signature of AAT geochemistry. The indicated 113 km by ~1300 km terrain ‘swath’ (~146.9 x 10^3 km^2) on the far side of Earth from the central AAT strewn field region represents a mere ~0.0288% of Earth’s ~509.6x10^6 km^2 total surface area, a relatively precise constraint on AAT source area possibilities. Within the indicated swath, Lake Huron (~59.59 x 10^3 km^2) is suggested. This is largely due to its contemporary geographic layout and bathymetry being a match to assumed cosmic KE partitioning signature of tektite ***A***-to-***B*** suborbital trajectories from there to each known fall point, ablated or otherwise, explaining the AAT imprint at the formative MIS 20 event epoch.

Lake Huron’s area is roughly 40% of the indicated source swath area, or ~0.0117% of Earth’s surface. Its area is slightly larger than a 250 km diameter (49,087 km^2) circular approximation of the buried Chicxulub crater, while deceptively ‘flat’ in relief by comparison. Ice sheet involvement over what is now Lake Huron explains the quizzical indication, providing expanding steam plasma as an escape route (literally) from Earth’s setting for much of the partitioned KE (synonymous with *heat*). The key to rationalizing the Lake Huron AAT source concept will come in part via assessment of transport KE required to move the estimated mass of AAT melt to the indicated speeds, and similarly albeit more-so to move the conformal blanket described in Davias, Harris (2022), even for the lower indicated transport speed of that blanket.

The estimated AAT tektite mass of 30 to 60 billion tons equates to roughly 0.17 km^3 of silicate melt propelled to ~10 km/s as a rough order-of-magnitude baseline. The N. American conformal blanket mass compares to something between 1600 and ~5000(?) km^3 of primarily silicate aggregate, propelled to ~3 or 4 km/s as assessed on a suborbital basis. The blanket mass and distribution represent several orders of magnitude more KE implied for transport, consistent with impact excavation that tends to produce larger volumes of outflow across decreasing range from the impact, i.e., inverse power law with blanket thickness proportional to $1/r^x$, where r is radius from the impact structure (consistent with observed proximal ejecta for more-circular impact structures). The giant scale of the N. American conformal aggregate blanket of Davias, Harris (2022) compares well with the uniquely large scale of AAT strewnfield mass and geographic area.

[Calling All Nuclide Geochemists…]

New findings of such aggregate blanket deposits continue to appear within the research, such as Rovey (2023) ‘An upland gravel complex in West Plains, Missouri (GSA Annual Meeting abstract & poster), making blanket volume accounting an ongoing task. Rovey (2023) places a 7-meter thickness of allochthonous aggregate in southern Missouri with "…contrast between the advanced state of chemical stability of the clasts and the textural immaturity (being) enigmatic”. Further per that reporting, “The quartzite seems to include both metamorphic and sedimentary varieties…” while the imagery depicted is reminiscent of a typical Michigan Basin assemblage. It is a scene from a Michigan beach. Cosmic nuclide chronology across the lower contact of these indicated conformal blanket emplacement examples should help with temporal constraint and to establish geographic bounds of the blanket.

The indicated Great Lakes region as an AAT source is challenging for scaling due to the relatively undefined boundaries of involvement at MIS 20, as well as the implied Laurentide Ice Sheet LIS (thick) overburden and possible seismic coupling to destabilize and comminute adjoining hydrated lobate basins of consolidated sediments through an arcuate range around Lake Huron (i.e., the Great Lakes complex).

These Supplements provide a synopsis of the overall suborbital transport paradigm, albeit somewhat simplified based on the first-order inverse-square gravity model that neglects higher order effects derived from 1) launch acceleration profiles, 2) dispersal through rarefaction of jetting phenomenon, 3) lessor orbital forcing factors of lunar gravity, solar wind, oblate Earth and gravity variation 4) a majority of reentry specifics, terminal descent profiles and ocean current effects (i.e., for μ-tektites), and probably a few others. It is a basic first-order assessment of AA tektite transport, and does not claim to be anything more. First-order accounting of partitioned astronomic KE from a cosmic impact at the AAT source region is the goal of this work. The presented review of the N. American source vs. anywhere in the S. E. Asia region succeeds in that regard.

Mizera et al. (2016) and Mizera (2022d) explain a relatively low Chemical Index of Alteration (CIA) required with the precursors to produce the observed AAT melt. This is typically the opposite of surface sediments and soils anywhere in the tropics, but supports a mid-latitude source scoured by continental ice sheet cycling leading up to the mid Pleistocene tektite-producing impact event. Further, while S. E. Asia and particularly Thailand, Khorat plateau has a conformal catastrophic emplacement of ~200 km^3 per Trnka, Tilsar (2021), there is no regional indication of an excavated astrobleme of comparable volume. On the other hand, the Thailand emplaced blanket compares well as a more distal component of the N. American blanket that bears at least an order of magnitude more volume, with S. E. Asia squarely in the downrange direction of the indicated oblique impact suggested by Lake Huron's layout per Figures 5(c) and 9(a) of this submission.

Intuitive Versus Factual Relationships of Impact Ejecta Transport

When considered together with NASA regional tektite ablation data across the AAT strewnfield, the detailed reporting within Tada et al. (2022) is telling. The tektite-bearing laterite-capped unit 2 of that work, undissected in the high-erosion tropical setting and (quickly) covered by subsequent unit 3 of fining-upward pure quartz sand (allochthonous to the setting), bears strong supporting evidence of the formative event taking place somewhere *significantly further North* (low CIO precursor of AAT melt) and *substantially up-spin* (to the East) across Earth's surface from S. E. Asia (indicated tektite loft was many hours, i.e., significant fraction of a day or a full Earth rotation), as demonstrated by the presented body of evidence and various known relationships of the physical sciences. Not all of these relationships are intuitive, suborbital analysis being a *perfect* example. The presented findings require acceptance of tektites as purely distal melt ejecta launched at the highest speed and earliest time in the causal event outflow, per definition of this relatively rare form of planetary impact ejecta. We must be careful as Kinetic Energy auditors to properly account for known facts. Tektites as purely distal ejecta is one of several facts we must accept in the proposed hypothesis.

Layered 'Moung Nong-type' AA tektites are sometimes considered as sourced from deeper in the target column and ejected at lower speeds later in the excavation phase. The more consistent (and accurate) definition places their origin as near-surface, ejected just as rapidly as other Indochinite AAT, based on compositional properties of hydration, vacuum devolatized lack of H_2O component, and $^{26}Al/^{10}Be$ cosmogenic nuclide ratio evidence. *None* of the Indochinite tektite varieties indicate significant excavation depths of any more than 1 or 2 meters to suggest they are more proximal ejecta. This is critical when considering that the AAT strewnfield covers roughly one quarter of Earth's surface, by far the largest known tektite strewnfield. Indochinite AA tektites went to space and solidified there, just like the rest of the observable AAT mass. Some contorted Indochinite morphologies exhibit plastic deformation during solidification, or post-solidus brittle fracture overprinted by the former, may be explained more consistently when considering other features of the AAT imprint, while any S. E. Asia source fails that bar due to the above-mentioned tektite composition trends.

The first continental landmass *significantly further North* and *substantially up-spin* of S. E. Asia is North America, which was covered by the Laurentide Ice Sheet at the AAT formative epoch of MIS 20. A disrupted ice sheet explains many observed features of the AAT imprint and the larger mid Pleistocene geologic record. This is jumping ahead of the accounting for regional ablation trends that indicate reentry speeds and vertical angles for ablated AA tektites found further South in the AAT stewnfield. AAT ablation trends cannot be explained by any S. E. Asia AAT source, leading us to another problem with legacy consensus in the AAT mystery.

The Baby Versus the Bathwater

A stumbling point of any S. E. Asia AAT source is the lack of trust or understanding of NASA’s 1960’s tektite ablation research. The NASA work led by Dr. Dean R. Chapman during President Kennedy’s lunar mandate enabled development of the heat transfer equation for hypervelocity upper atmospheric entry, from free-molecular flow regime (i.e., the ‘exosphere’) into lower, collisional flow regime (crossing the ‘exobase’). This equation, called the “Chapman equation” for its developer, is essentially a blended or ‘splined’ curve fit between heat transfer properties of the two flow regimes. Coefficients of the curve fit are derived by reproducing ablated tektite morphologies using tektite glass during extensive hypervelocity plasma arc jet wind tunnel testing to reproduce the range of conditions during hypervelocity atmospheric entry. The Chapman equation was then used to develop the Apollo lunar mission heat shield design, which proved robustly reliable thanks to the extensive testing to reproduce ablated shapes of the natural tektite specimens. The researchers got it right, which is important to understand in this case. It requires belief that we put astronauts on the Moon and repeatedly delivered them safely back to Earth.

Unfortunately, Dr. Chapman omitted a critical rotating frame transformation as detailed in Harris (2022) when trying to assess the inverse suborbital problem, as explained in Section 1 (Historic Framing) of this manuscript. Rotating frame dynamics was not his strong suit, while success or failure of the Apollo manned lunar missions definitely did depend on his aerothermodynamics derivation. His error of omission invalidates the resulting 'lunar origin' hypothesis, while being completely independent of the highly reliable ablation data. Naturally the bad result (lunar origin of tektites) wasn't fully realized until advancing compositional analysis, nuclear chemistry and electric microscopy over subsequent decades allowed lunar samples from 1969 through the early 1970s to be acknowledged as AAT precursor *non-starters*. Chapman's error of omission and subsequent lunar origin hypothesis represent an insignificantly small failure in the larger success of brilliant Apollo mission results, while trust in the highly reliable ablation data was undermined within the geoscience camp. The baby was thrown out with the bathwater, so to speak. This was a setback to the AAT source identification, while also fostering a large body of compiled details on tektite composition, distribution and morphologic constraints, all of which are pivotal within the presented research.

This manuscript uses the NASA-derived tektite ablation data and suborbital analysis to calculate possible vs. impossible source regions for the AAT across Earth’s surface, the inverse suborbital problem or “Chapman problem” so called within. The Chapman problem is a variation of the ***A***-to-***B*** suborbital problem, where the inverse suborbital ballistic paradigm allows solutions of ‘***A***-given-***B***’ instead. Inverse solutions are possible because the simplified version of the governing equation is mechanically conservative, with specific mechanical energy of an orbit (or sub-orbit) being constant, and elliptical trajectory segments having major axis through Earth’s center. Mathematically, it is a second-order governing differential equation with no first-order ‘damping’ term, meaning that no energy is lost during suborbital transit of the tektites in the first approximation. Their launch condition is symmetric with their fall condition. This also means that the solutions of the ***A***-given-***B*** suborbital problem are piecewise continuous and may be resolved by various mathematical means, including iteration with nothing more than the ‘Goal Seek’ solver of modern spreadsheets, as long as careful choices of initial conditions and algorithms are employed. The supplemental results presented have extensive automated solutions of this type, all performed on a desktop computer with commonly available consumer software.

Automation is not necessary to check random pieces of the presented solutions, while those codes are contained in the Visual Basic editor attached to the spreadsheet suborbital solver tools. In their basic form as delivered, the solvers operate as simple spreadsheets only, and already contain the presented solutions as output listings on various sheets or 'workbook pages'. Activating any of the macro segments is only advisable for experienced computer users using an isolated machine in well-backed-up condition. Macro coding work does have a tendency to 'hang' the computer and require a soft or hard reset as a result. Look for the user guide and support file of Harris (2022) when attempting to reproduce any of this work. And as always when practicing computer science and code development, "save early and often."

Symmetry about the trajectory ellipse axis, the "line of nodes" in astrodynamics language, combined with Kepler's constant orbital sweep-area-per-time law and some gravitational constants, allows time-of-flight calculation. Known time-of-flight or 'loft duration' permits fall point longitude calculation across the rotating Earth's surface based on launch location and launch vector definition (launch conditions). For launch speed below Earth's escape speed (<11.175 km/s), the set of these launch location and condition input variables defines the state of the suborbital trajectory, allowing fall point calculation as detailed in Harris (2022).

Luckily, the 1960s NASA tektite ablation regime data derived for different AAT fall regions equate directly to the suborbital variables of launch/fall elevation angle and launch/reentry speed, the key to solution of the ***A***-given-***B*** inverse suborbital problem or 'Chapman problem'. The reader doesn't have to know these details because the Harris (2022) reference provides the suborbital solver spreadsheet as shareware. All that is required is a belief in physical science and dynamically correct accounting for the governing inverse-square gravity problem with coordinate transforms for the rotating Earth beneath the trajectory. Seek out the Harris (2022) reference and associated supplements for hours of user enjoyment.

Failed consensus in the form of an unlocated, large and geologically recent cosmic impact structure after 5+ decades indicates that many (most?) tektite researchers are either 1) unaware of the missing rotating frame conversion in the otherwise highly reliable tektite ablation data of the 1960s NASA tektite research (we repeatedly went to the Moon and returned safely based on this exact body of ablation research), or 2) unaware that launch speeds at substantial fractions of Earth's escape Kinetic Energy (KE) will substantially convolute ejecta fall patterns across Earth's surface, as elegantly described in Dobrovolskis (1981 - more than 4 decades ago), or 3) unaware of both of these facts. Five or six decades after NASA's tektite ablation research efforts, we now have the capacity to solve the AAT source region mystery.

Lack of trust in NASAs Australasian tektite ablation regime data is an unfortunate result considering the millions of dollars poured into that 1960s research. NASA Apollo mission results are a solid indication of ‘valid science’ to put things quite simply.

The problem was that nobody ever dug deep enough into the 1960s NASA research since then to recognize the devastating error of omission, so the missing bit of dynamical accounting went unreported while at once invalidating the ‘Lunar Origin’ hypothesis for tektites. This author found the repeated error of omission in 2016-2017 after five years of continuous searching based on a gut feeling form professional experience as an orbit analyst in the defense aerospace sector, and a lifetime of diverse exposure in the physical sciences. The extent of the described failed consensus is what happens when errors of omission go unnoticed in critical bodies of research. It is a serious issue, and the longer the error resides, the more painful the recounting process becomes. The difference in results is as clear as one side of the planet versus the other side, and also compare to the difference between the far side of Earth versus the Moon as the AAT source region and its distance from the center of the AAT strewnfield. It really is that simple.

Further explanation of the presented data is provided in each individual Supplement.

Supplements S1.

Huai Om and the Indochina Suborbital Situation

Helix suborbital solver results for 1^{st}- and 2^{nd}-way suborbital trajectories from Huai Om, Thailand to the Central Indian Ocean Basin (CIO) button tektite fall site, 14.579°N, 105.275°E To -12.61°N, 78.50°E are presented in Figure S1(a).

The no-ring-waves dynamic pressure upper limit per Chapman, Larson (1963) and Chapman (1964) of 0.25 atmospheres (Atm) intersects measured CIO ablation bounds at ~23° launch EL, and Glass, Chapman, Prasad (1996) estimate the EL upper limit: (p367, l/h column, "…restricted to trajectories with gamma$_i$ <~20° to 30° [Chapman and Larson 1963])". Flight path angle Gamma$_i$ from horizontal at initial reentry is synonymous with launch EL via suborbital symmetry. Figure S1(a) shows this range of launch EL marginally intersecting the CIO button ablation regime via 2^{nd}-way trajectory only, a possibility Chapman was apparently unaware of.

Helix solutions to the CIO button fall site from Indochina E-W and N-S limits in Figure S1(a) are curves with no markers next to 1^{st}-way and 2^{nd}-way baseline Huai Om curves with markers, the lot being unlikely candidates to produced observed CIO button ablation. The Lat/Long ranges considered as surrounding Indochina are 8.25° to 23.5° N and 97° to 109.5°E, providing some margin while also revealing the inadequacy of the overall region as an AAT source due to ablation-derived suborbital transport restrictions. Indochina is a bad source region match for observed ablation of the CIO button tektite in Glass, Chapman, Prasad (1996).

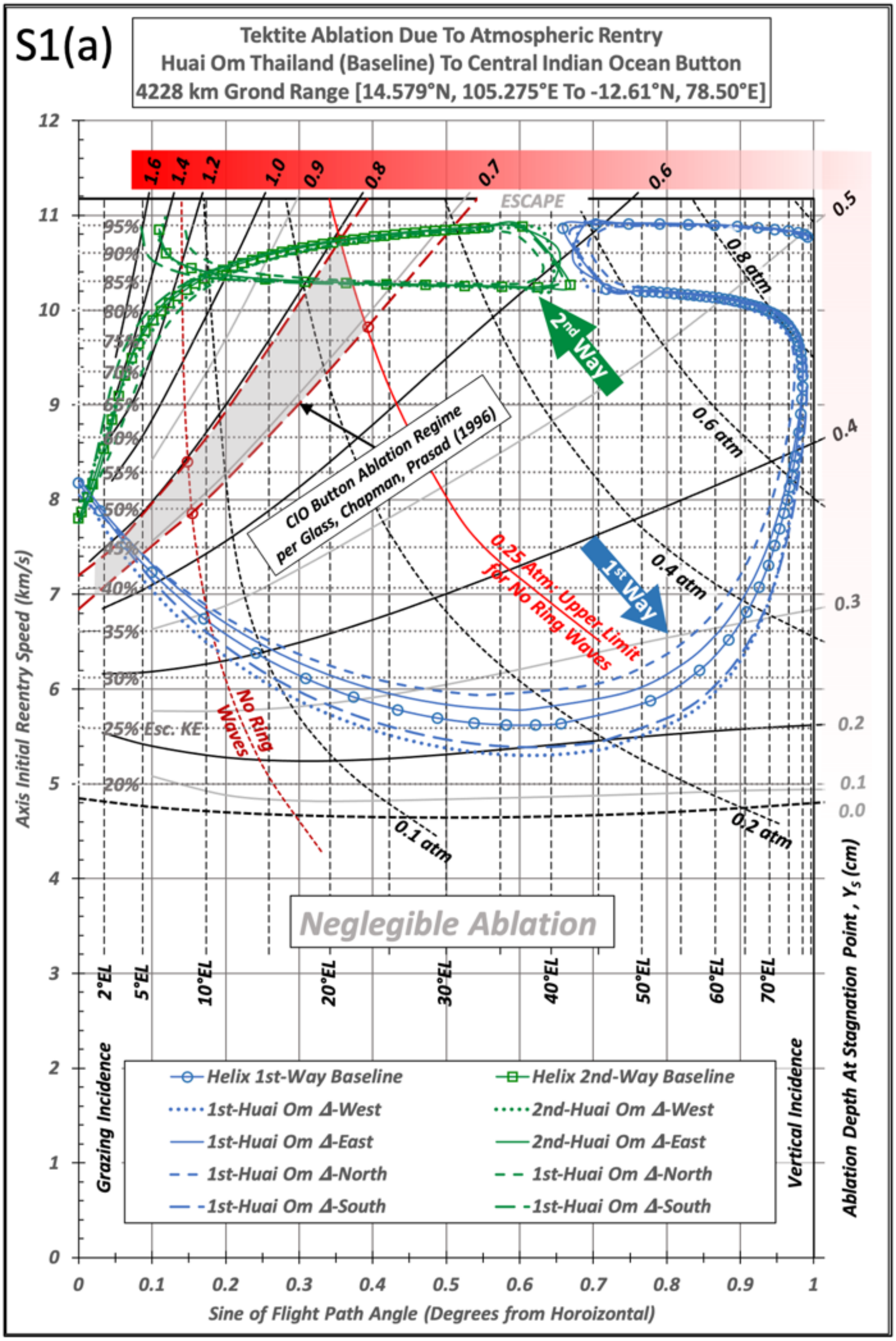
S1(a)
Tektite Ablation Due To Atmospheric Rentry
Huai Om Thailand (Baseline) To Central Indian Ocean Button
4228 km Grond Range [14.579°N, 105.275°E To -12.61°N, 78.50°E]
ESCAPE
CIO Button Ablation Regime per Glass, Chapman, Prasad (1996)
2nd Way
1st Way
0.25 Atm-Upper Limit for No Ring Waves
No Ring Waves
0.8 atm
0.6 atm
0.4 atm
0.2 atm
0.1 atm
Neglegible Ablation
25% Esc. KE
2°EL
5°EL
10°EL
20°EL
30°EL
40°EL
50°EL
60°EL
70°EL
Grazing Incidence
Vertical Incidence
Helix 1st-Way Baseline
Helix 2nd-Way Baseline
1st-Huai Om Δ-West
2nd-Huai Om Δ-West
1st-Huai Om Δ-East
2nd-Huai Om Δ-East
1st-Huai Om Δ-North
1st-Huai Om Δ-North
1st-Huai Om Δ-South
1st-Huai Om Δ-South
Axis Initial Reentry Speed (km/s)
Sine of Flight Path Angle (Degrees from Horoizontal)
Ablation Depth At Stagnation Point , Y_S (cm)

Figure S1(a). *Ablation regime diagrams including this one are reconstructed from 1960s NASA tektite ablation research reported in Chapman, Larson (1963) and Chapman (1964). That work used naturally ablated tektite specimens to derive coefficients of the "Chapman equation" for hypervelocity entry into Earth's upper atmospheric column. The Chapman equation was pivotal in Apollo lunar mission heat shield design, which proved robustly reliable thanks to the extensive hypervelocity arc jet testing by NASA's ablation research team led by Chapman. 1st and 2nd-way solution families from Helix suborbital solver of Harris (2022) from Huai Om, Thailand to the Central Indian Ocean (CIO) button tektite fall site cross the shaded ablation regime of that specimen at marginal far upper and far left regions only, indicating S. E. Asia as an unlikely Australasian tektite (AAT) source region, despite legacy consensus to the contrary. Curves with markers are from Huai Om, while neighboring curves with no markers represent suborbital launch or 'ejection' from the latitude and longitude limits of the Indochina region. The ablation regime crossings are essentially the same, all marginal, corner-crossing of the regime (no ridgeline crossing) or indicated at launch elevation angles of 5° or less.*

The Glass, Chapman, Prasad (1996) narrative considers "*a hypothetical source area in Indochina (Stauffer, 1978)*", while realizing launch EL from Indochina "…*must have been shallow (only a few degrees) and its velocity on the order of 7 km/s.*" This is a good assessment of a 1^{st}-way trajectory possibility per Figure S1(a), showing 1^{st}-way ablation regime crossing at < 5° EL, while ever-lower EL values become geometrically less likely from a physical mechanics standpoint. (A dual-impulse scenario is required to make a near-circular low-EL orbit or suborbital trajectory above Earth's atmosphere from any surface launch.) The transport assessment of Glass, Chapman, Prasad (1996) ignores possible 2^{nd}-way options that marginally traverse the CIO ablation regime (upper right corner), where (unobserved) anterior ring waves are admittedly more probable.

In any case, invoking *Stauffer (1978)* in this mid 1990s work is a telling indication that any solid grasp on the terrestrial suborbital paradigm was lacking in terms of rotating frame transformation requirements, thus the clear need for the present effort. Our speculations must always be informed and bounded by physical mechanics realities. Lastly, unexpected higher levels of $Na_2$0 and $K_2$0 on the *anterior* (ablation-melted) CIO button surface per Glass, Chapman, Prasad (1996) (p366) may indicate elevated levels of those volatiles in the descent corridor during swarm reentry per suggestions of Prasad, Khedekar (2003). The CIO button composition resembled high-Mg australites such as those found in Serpentine Lakes and Lake Wilson in S. Australia. These are excellent observations for the overall mystery, suggesting that the high-Mg compositional sub-family of AAT melt was ejected together in a southerly directed jetting pulse, as explored further in Section 4.

Supplement S2.

Inverse Suborbital Solutions for the Indochina Fall Site – Constant KE

Curves of constant launch Kinetic Energy (~synonymous with constant launch speed) to reach Huai Om Thailand at various launch elevation angles (EL) and launch azimuths indicated by direction vectors along the curves (‘AZ vecs’).

Inverse Suborbital Solutions for the Indochina Fall Site – Constant EL

Inverse suborbital solutions (***A***-given-***B***) of this supplement represent launch solution curves across the global landscape for launch conditions to reach Huai Om, Thailand, a representative of legacy consensus for the Australasian tektite (AAT) source somewhere in S. E. Asia. Huai Om is chosen for being well-documented in Tada et al. (2022). While many other S. E. Asia AAT source locations have been hypothesized in the literature over the decades, one or another location within this central region of the giant AAT strewnfield make little difference in the larger picture of dynamically correct possible source regions.

Supplement S1 results are meant to show that any source near the S. E. Asia region doesn’t provide a match for the definition of the vacuum devolatilized, vacuum quenched impact ejecta melt glass (tektites, per definition) because the plastic deformation seemingly induced in a semi-solidus state is actually imprinted atop brittle fracture features, a condition indicative of post-solidus material properties in a significant fraction of Indochinite fragment-form (or ‘irregular’ or ‘tektite waste’) samples, further elaborated in Supplement S4.

Brittle fracture planes of fragmented Indochinite spheroidal shapes are further contorted through plastic deformation, while electro-magnetic (EM) field lines are apparently imprinted as surface striae, consistent with high-voltage (HV) arcing along the indicated fracture axes. This explains observed morphologies via in-transit EM processes versus often-suggested atmospheric entry disruption proposed or suggested in earlier references such as Barnes (1959) and many S. E. Asia AAT source consensus works. Indochinites AA tektites didn't land in molten or in semi-solidus plastic condition. They were solid. Many of them are deformed beyond what they should be from solely in-vacuum transport and reentry effects. Explaining those features is an important portion of this work. Figure 10(e) provides classic evidence of post-solidus reentry reheating of spheroidal Indochinite thin outer layer, a typical observation when attempting to cut those types.

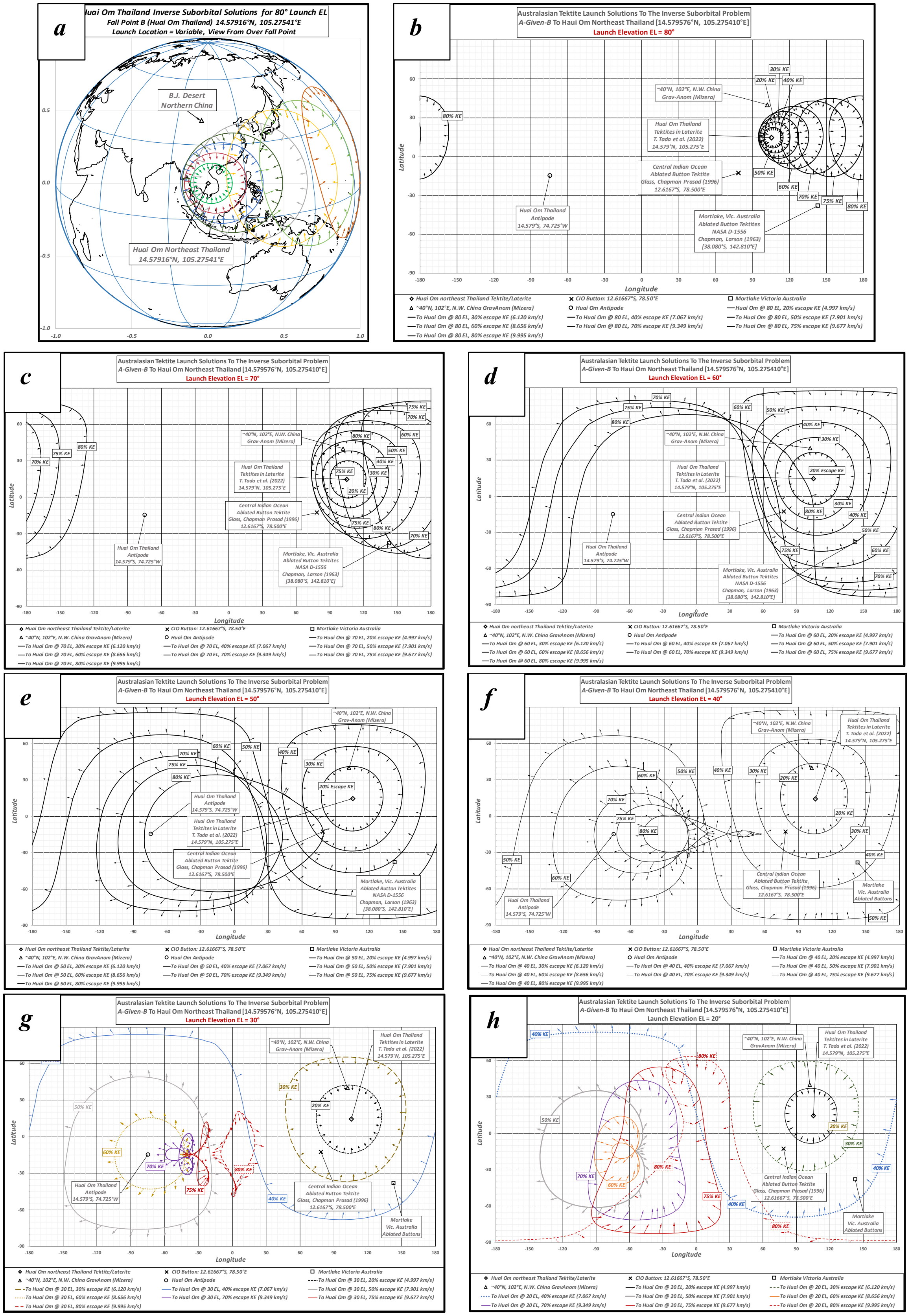
a
Huai Om Thailand Inverse Suborbital Solutions for 80° Launch EL
Fall Point B (Huai Om Thailand) 14.57916°N, 105.27541°E
Launch Location = Variable, View From Over Fall Point
B.J. Desert
Northern China
Huai Om Northeast Thailand
14.57916°N, 105.27541°E
b
Australasian Tektite Launch Solutions To The Inverse Suborbital Problem
A-Given-B To Haui Om Northeast Thailand [14.579576°N, 105.275410°E]
Launch Elevation EL = 80°
~40°N, 102°E, N.W. China
Grav-Anom (Mizera)
Huai Om Thailand
Tektites in Laterite
T. Tada et al. (2022)
14.579°N, 105.275°E
Central Indian Ocean
Ablated Button Tektite
Glass, Chapman Prasad (1996)
12.6167°S, 78.500°E
Huai Om Thailand
Antipode
14.579°S, 74.725°W
Mortlake, Vic. Australia
Ablated Button Tektites
NASA D-1556
Chapman, Larson (1963)
[38.080°S, 142.810°E]
Latitude
Longitude
Huai Om northeast Thailand Tektite/Laterite
~40°N, 102°E, N.W. China GravAnom (Mizera)
CIO Button: 12.61667°S, 78.50°E
Huai Om Antipode
Mortlake Victoria Australia
To Huai Om @ 80 EL, 20% escape KE (4.997 km/s)
To Huai Om @ 80 EL, 30% escape KE (6.120 km/s)
To Huai Om @ 80 EL, 40% escape KE (7.067 km/s)
To Huai Om @ 80 EL, 50% escape KE (7.901 km/s)
To Huai Om @ 80 EL, 60% escape KE (8.656 km/s)
To Huai Om @ 80 EL, 70% escape KE (9.349 km/s)
To Huai Om @ 80 EL, 75% escape KE (9.677 km/s)
To Huai Om @ 80 EL, 80% escape KE (9.995 km/s)
c
Australasian Tektite Launch Solutions To The Inverse Suborbital Problem
A-Given-B To Haui Om Northeast Thailand [14.579576°N, 105.275410°E]
Launch Elevation EL = 70°
d
Australasian Tektite Launch Solutions To The Inverse Suborbital Problem
A-Given-B To Haui Om Northeast Thailand [14.579576°N, 105.275410°E]
Launch Elevation EL = 60°
e
Australasian Tektite Launch Solutions To The Inverse Suborbital Problem
A-Given-B To Haui Om Northeast Thailand [14.579576°N, 105.275410°E]
Launch Elevation EL = 50°
f
Australasian Tektite Launch Solutions To The Inverse Suborbital Problem
A-Given-B To Haui Om Northeast Thailand [14.579576°N, 105.275410°E]
Launch Elevation EL = 40°
g
Australasian Tektite Launch Solutions To The Inverse Suborbital Problem
A-Given-B To Haui Om Northeast Thailand [14.579576°N, 105.275410°E]
Launch Elevation EL = 30°
h
Australasian Tektite Launch Solutions To The Inverse Suborbital Problem
A-Given-B To Haui Om Northeast Thailand [14.579576°N, 105.275410°E]
Launch Elevation EL = 20°

Figure S2. ***Constant Kinetic Energy (KE)*** *inverse suborbital launch solutions to Huai Om Thailand for 10° launch elevation (EL) increments from 80° through 20° are presented in Frames (a) through (h) respectively, each depicting 10% launch Kinetic Energy (KE) in increments from 20% through 80% as calculated using SASolver of Harris (2022), described in Section 2 of the main text. Frames (a) and (b) are the same case, with (a) showing the GlobeView version of that reference (available as shareware and linked in the References section) while Frame (b) and subsequent Frames use a rectangular projection to provide all data of each EL case in a single frame.*

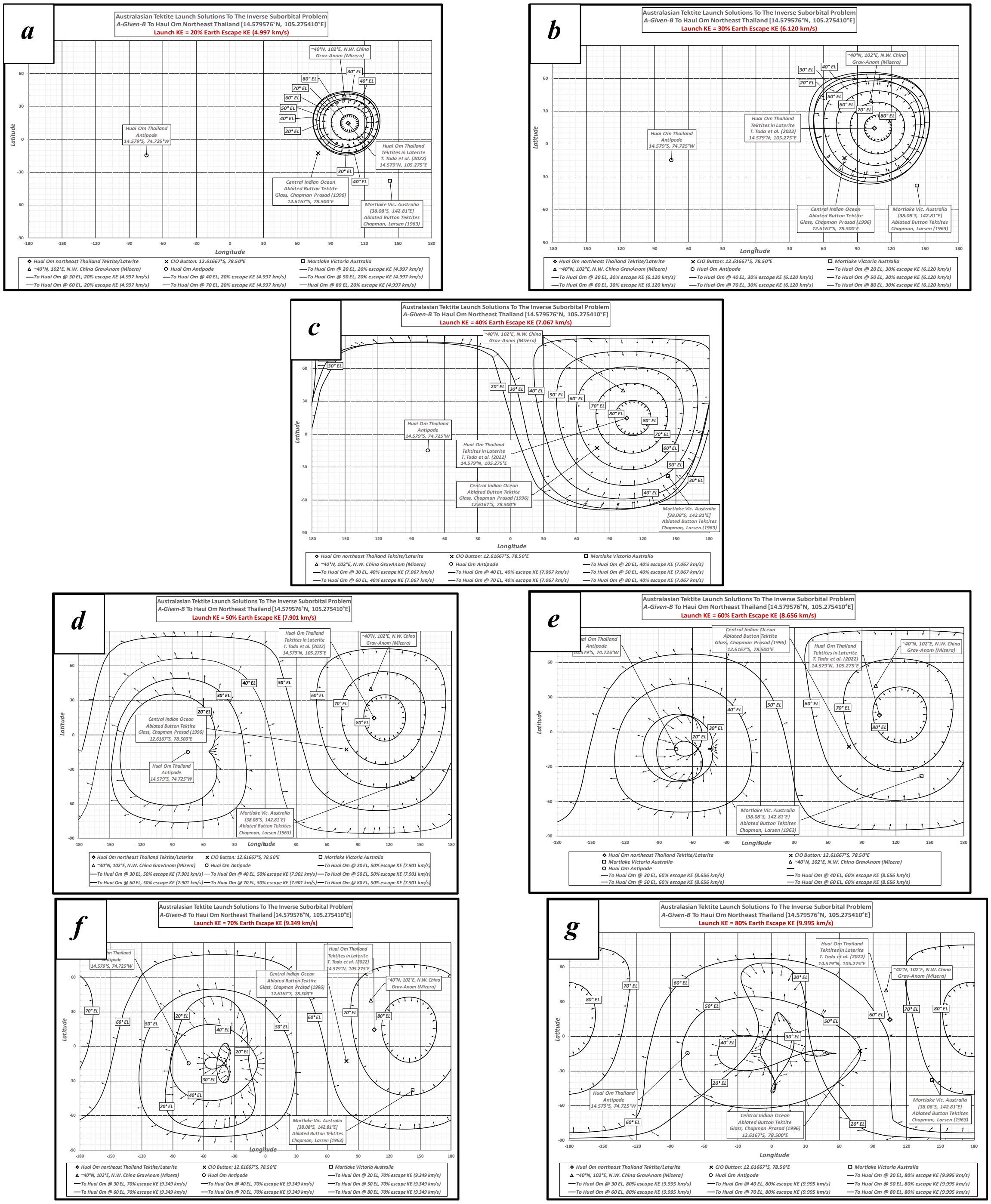
a
Australasian Tektite Launch Solutions To The Inverse Suborbital Problem
A-Given-B To Haui Om Northeast Thailand [14.579576°N, 105.275410°E]
Launch KE = 20% Earth Escape KE (4.997 km/s)
b
Australasian Tektite Launch Solutions To The Inverse Suborbital Problem
A-Given-B To Haui Om Northeast Thailand [14.579576°N, 105.275410°E]
Launch KE = 30% Earth Escape KE (6.120 km/s)
c
Australasian Tektite Launch Solutions To The Inverse Suborbital Problem
A-Given-B To Haui Om Northeast Thailand [14.579576°N, 105.275410°E]
Launch KE = 40% Earth Escape KE (7.067 km/s)
d
Australasian Tektite Launch Solutions To The Inverse Suborbital Problem
A-Given-B To Haui Om Northeast Thailand [14.579576°N, 105.275410°E]
Launch KE = 50% Earth Escape KE (7.901 km/s)
e
Australasian Tektite Launch Solutions To The Inverse Suborbital Problem
A-Given-B To Haui Om Northeast Thailand [14.579576°N, 105.275410°E]
Launch KE = 60% Earth Escape KE (8.656 km/s)
f
Australasian Tektite Launch Solutions To The Inverse Suborbital Problem
A-Given-B To Haui Om Northeast Thailand [14.579576°N, 105.275410°E]
Launch KE = 70% Earth Escape KE (9.349 km/s)
g
Australasian Tektite Launch Solutions To The Inverse Suborbital Problem
A-Given-B To Haui Om Northeast Thailand [14.579576°N, 105.275410°E]
Launch KE = 80% Earth Escape KE (9.995 km/s)
Latitude
Longitude

Figure S3 ***Constant launch elevation (EL)*** *inverse suborbital launch solutions to Huai Om Thailand for 10% escape KE increments from 20% to 80% are shown in Frames (a) through (g) respectively, each with 10° launch elevation (EL) increments from 20° to 80°, again as calculated with 'SASolver' of Harris (2022) and described in the Computational Method section of the main text. Observed high-ablation and low launch EL indicated by low reentry dynamic pressure from lack of anterior ring waves of the Central Indian Ocean (CIO) button tektite of Glass, Chapman, Prasad (1996) means that the ablated button tektite could not have originated from Huai Om Thailand or the S. E. Asia region, according to known laws of suborbital mechanics and primary ablation observations from 1960s NASA research and the 1996 paper mentioned above.*

Supplement S4.

Figure S4. Each location with an ablation regime is examined for the N. American Great Lakes as a possible launch region, comparing *Helix* output from launch region to each of the tektite fall regions.

S4(a)

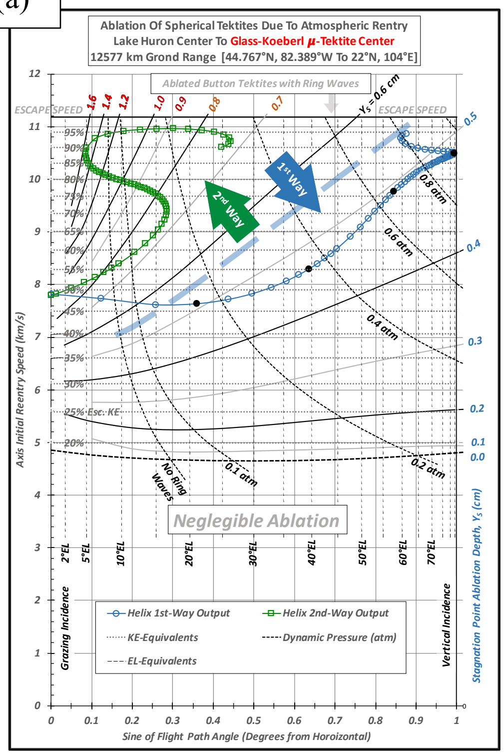

S4(a)2

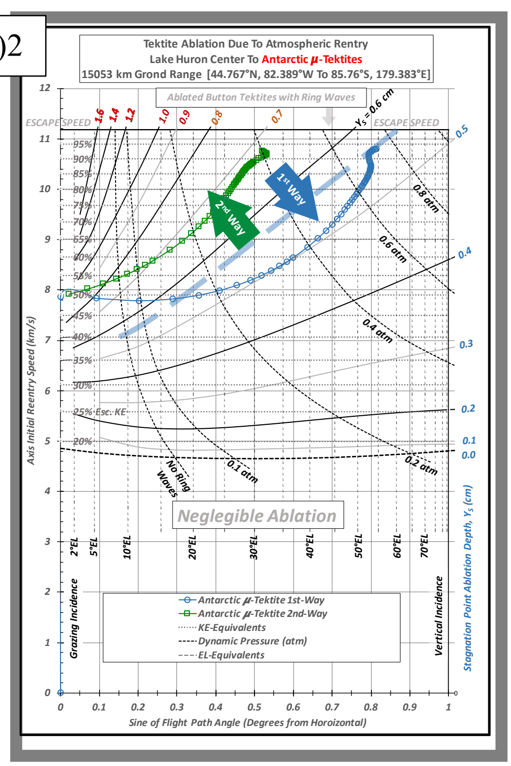

Figure S4 (continued). Frame 1 shows extended possibilities for ablation-limiting 1st-way suborbital trajectory solutions of more vertical reentry angles along the lower curve with circle markers, paralleling the thick dashed line labelled "A" on its lower-ablation side.

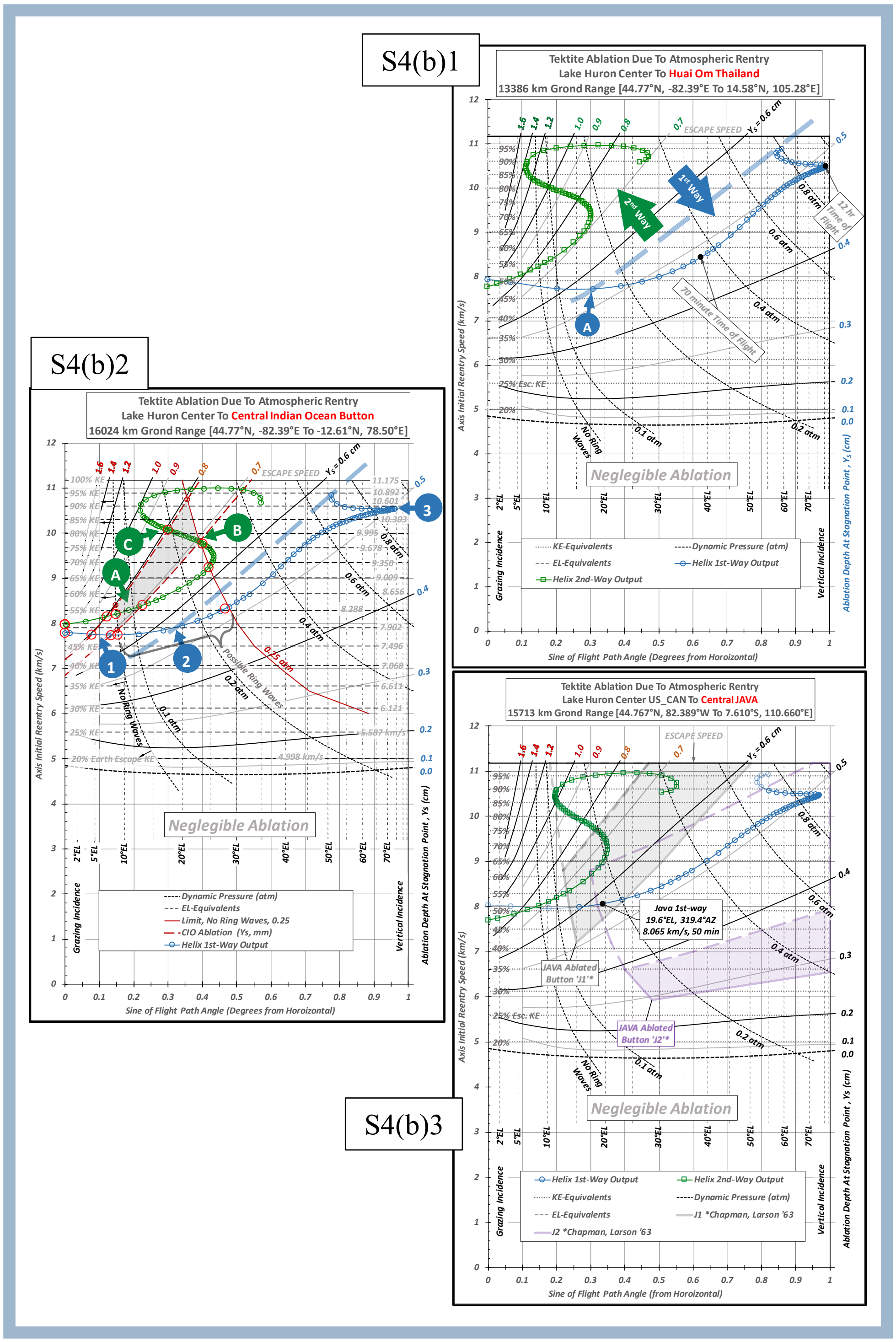

Figure S4 (continued)

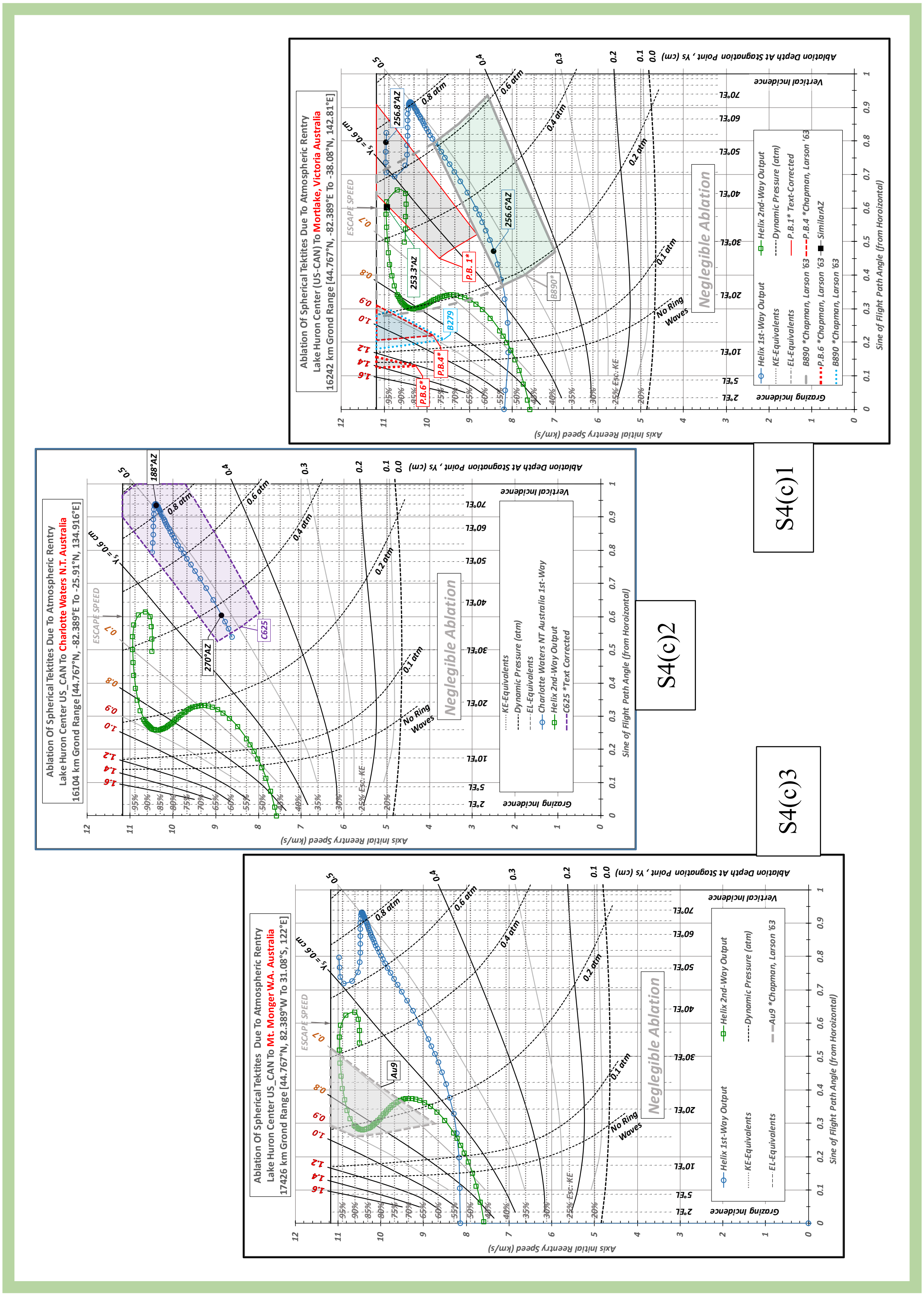

Lessor (non-primary) ablation regime windows are considered in the following diagrams. The windows are often too wide for discriminating any S. E. Asia source vs. a N. American source for the Australasian tektites.

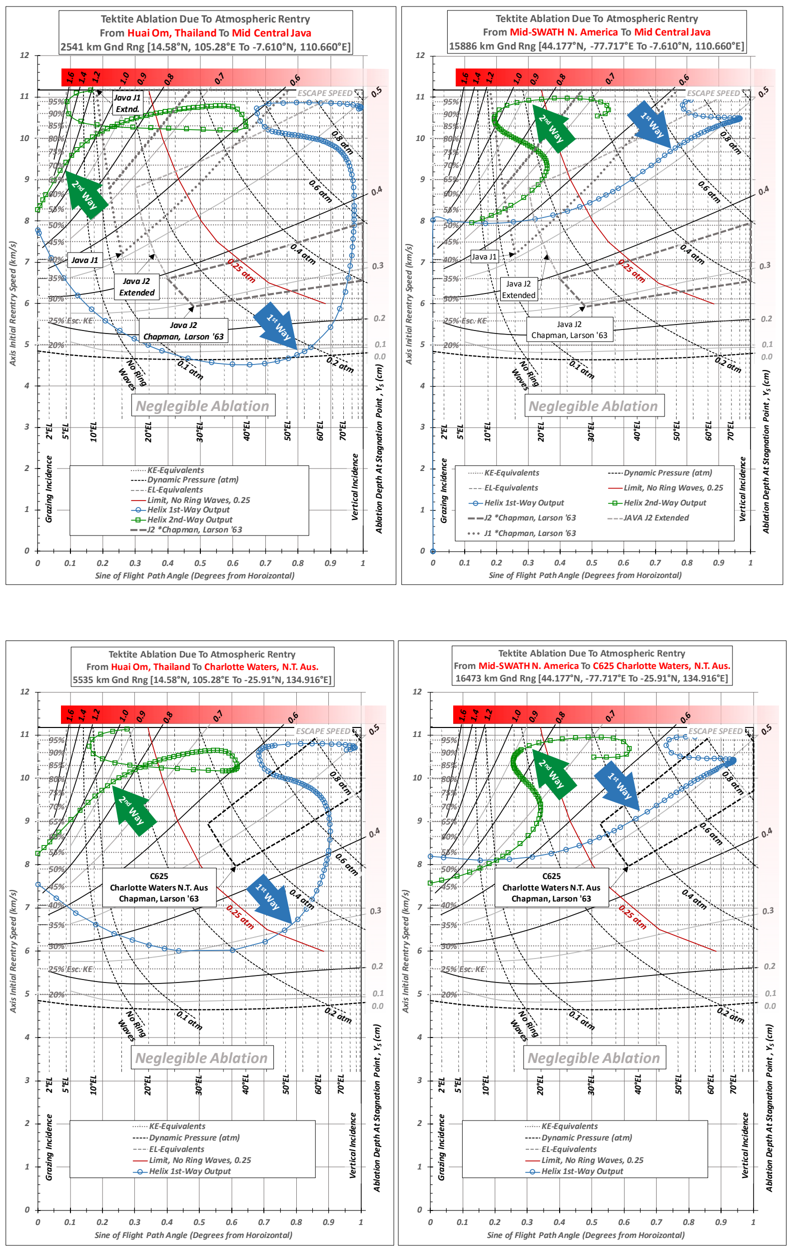

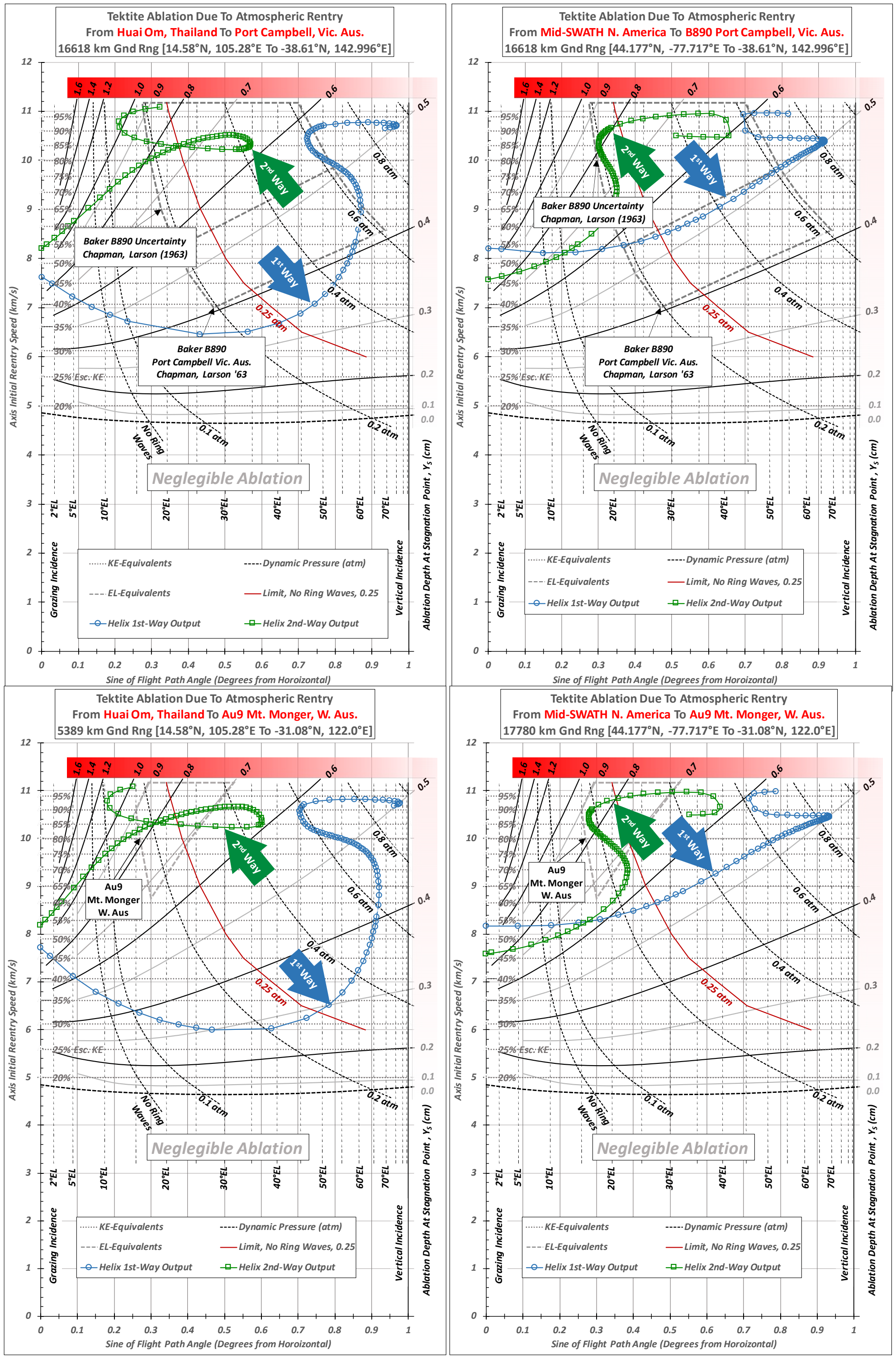

Tektite Ablation Due To Atmospheric Reentry
From Huai Om, Thailand To Port Campbell, Vic. Aus.
16618 km Gnd Rng [14.58°N, 105.28°E To -38.61°N, 142.996°E]
Baker B890 Uncertainty Chapman, Larson (1963)
Baker B890 Port Campbell Vic. Aus. Chapman, Larson '63
Tektite Ablation Due To Atmospheric Reentry
From Mid-SWATH N. America To B890 Port Campbell, Vic. Aus.
16618 km Gnd Rng [44.177°N, -77.717°E To -38.61°N, 142.996°E]
Baker B890 Uncertainty Chapman, Larson (1963)
Baker B890 Port Campbell Vic. Aus. Chapman, Larson '63
Tektite Ablation Due To Atmospheric Reentry
From Huai Om, Thailand To Au9 Mt. Monger, W. Aus.
5389 km Gnd Rng [14.58°N, 105.28°E To -31.08°N, 122.0°E]
Au9 Mt. Monger W. Aus
Tektite Ablation Due To Atmospheric Reentry
From Mid-SWATH N. America To Au9 Mt. Monger, W. Aus.
17780 km Gnd Rng [44.177°N, -77.717°E To -31.08°N, 122.0°E]
Au9 Mt. Monger W. Aus
1st Way
2nd Way
0.25 atm
0.1 atm
0.2 atm
0.4 atm
0.6 atm
0.8 atm
No Ring Waves
25% Esc. KE
Neglegible Ablation
KE-Equivalents
Dynamic Pressure (atm)
EL-Equivalents
Limit, No Ring Waves, 0.25
Helix 1st-Way Output
Helix 2nd-Way Output
Grazing Incidence
Vertical Incidence
Axis Initial Reentry Speed (km/s)
Ablation Depth At Stagnation Point, Y_S (cm)
Sine of Flight Path Angle (Degrees from Horoizontal)

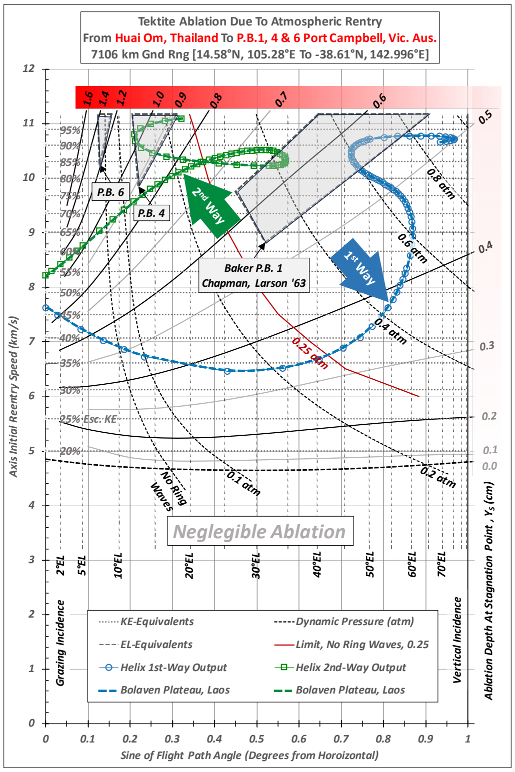

Tektite Ablation Due To Atmospheric Rentry
From Huai Om, Thailand To P.B.1, 4 & 6 Port Campbell, Vic. Aus.
7106 km Gnd Rng [14.58°N, 105.28°E To -38.61°N, 142.996°E]
Axis Initial Reentry Speed (km/s)
Sine of Flight Path Angle (Degrees from Horoizontal)
Ablation Depth At Stagnation Point , Y_S (cm)
Grazing Incidence
Vertical Incidence
Neglegible Ablation
Baker P.B. 1
Chapman, Larson '63
P.B. 6
P.B. 4
1st Way
2nd Way
No Ring Waves
KE-Equivalents
Dynamic Pressure (atm)
EL-Equivalents
Limit, No Ring Waves, 0.25
Helix 1st-Way Output
Helix 2nd-Way Output
Bolaven Plateau, Laos
Bolaven Plateau, Laos

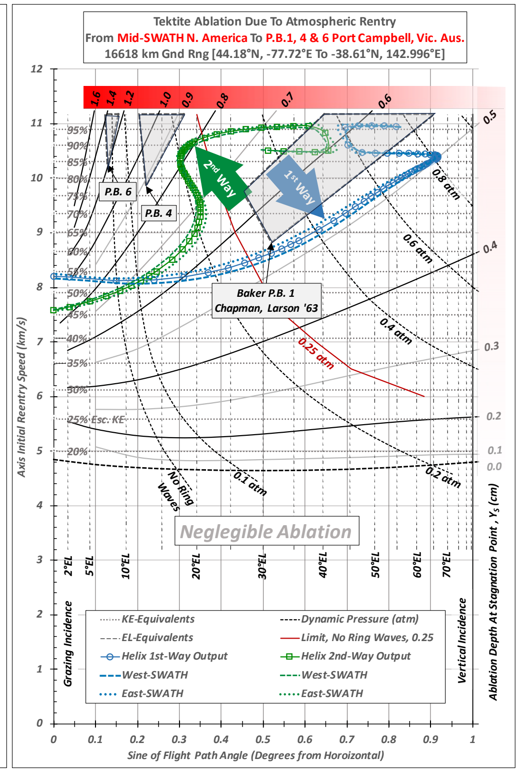

Tektite Ablation Due To Atmospheric Rentry
From Mid-SWATH N. America To P.B.1, 4 & 6 Port Campbell, Vic. Aus.
16618 km Gnd Rng [44.18°N, -77.72°E To -38.61°N, 142.996°E]
Axis Initial Reentry Speed (km/s)
Sine of Flight Path Angle (Degrees from Horoizontal)
Ablation Depth At Stagnation Point , Y_S (cm)
Grazing Incidence
Vertical Incidence
Neglegible Ablation
Baker P.B. 1
Chapman, Larson '63
P.B. 6
P.B. 4
1st Way
2nd Way
KE-Equivalents
Dynamic Pressure (atm)
EL-Equivalents
Limit, No Ring Waves, 0.25
Helix 1st-Way Output
Helix 2nd-Way Output
West-SWATH
West-SWATH
East-SWATH
East-SWATH

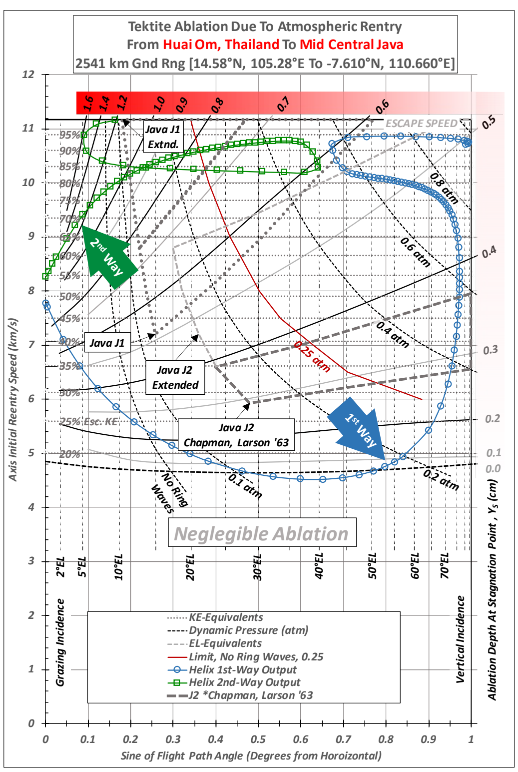

Tektite Ablation Due To Atmospheric Rentry
From Huai Om, Thailand To Mid Central Java
2541 km Gnd Rng [14.58°N, 105.28°E To -7.610°N, 110.660°E]
Axis Initial Reentry Speed (km/s)
Sine of Flight Path Angle (Degrees from Horoizontal)
Ablation Depth At Stagnation Point , Y_S (cm)
Grazing Incidence
Vertical Incidence
Neglegible Ablation
ESCAPE SPEED
Java J1 Extnd.
Java J1
Java J2 Extended
Java J2
Chapman, Larson '63
1st Way
2nd Way
KE-Equivalents
Dynamic Pressure (atm)
EL-Equivalents
Limit, No Ring Waves, 0.25
Helix 1st-Way Output
Helix 2nd-Way Output
J2 *Chapman, Larson '63

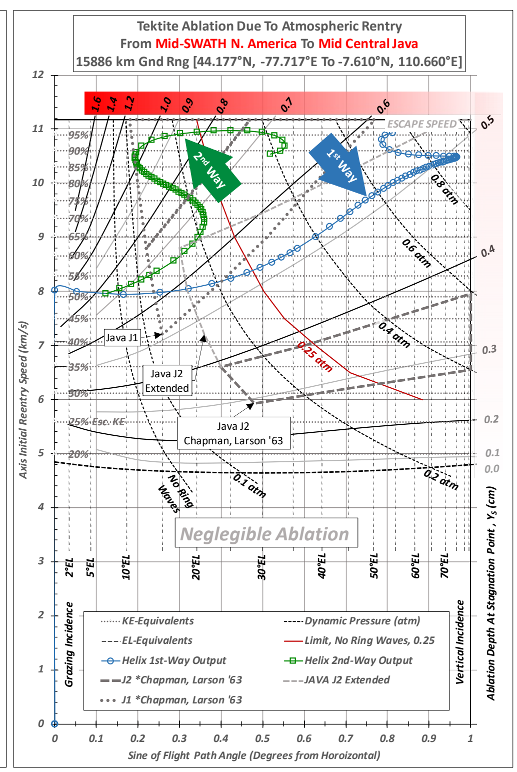

Tektite Ablation Due To Atmospheric Rentry
From Mid-SWATH N. America To Mid Central Java
15886 km Gnd Rng [44.177°N, -77.717°E To -7.610°N, 110.660°E]
Axis Initial Reentry Speed (km/s)
Sine of Flight Path Angle (Degrees from Horoizontal)
Ablation Depth At Stagnation Point , Y_S (cm)
Grazing Incidence
Vertical Incidence
Neglegible Ablation
ESCAPE SPEED
Java J1
Java J2 Extended
Java J2
Chapman, Larson '63
1st Way
2nd Way
KE-Equivalents
Dynamic Pressure (atm)
EL-Equivalents
Limit, No Ring Waves, 0.25
Helix 1st-Way Output
Helix 2nd-Way Output
J2 *Chapman, Larson '63
JAVA J2 Extended
J1 *Chapman, Larson '63

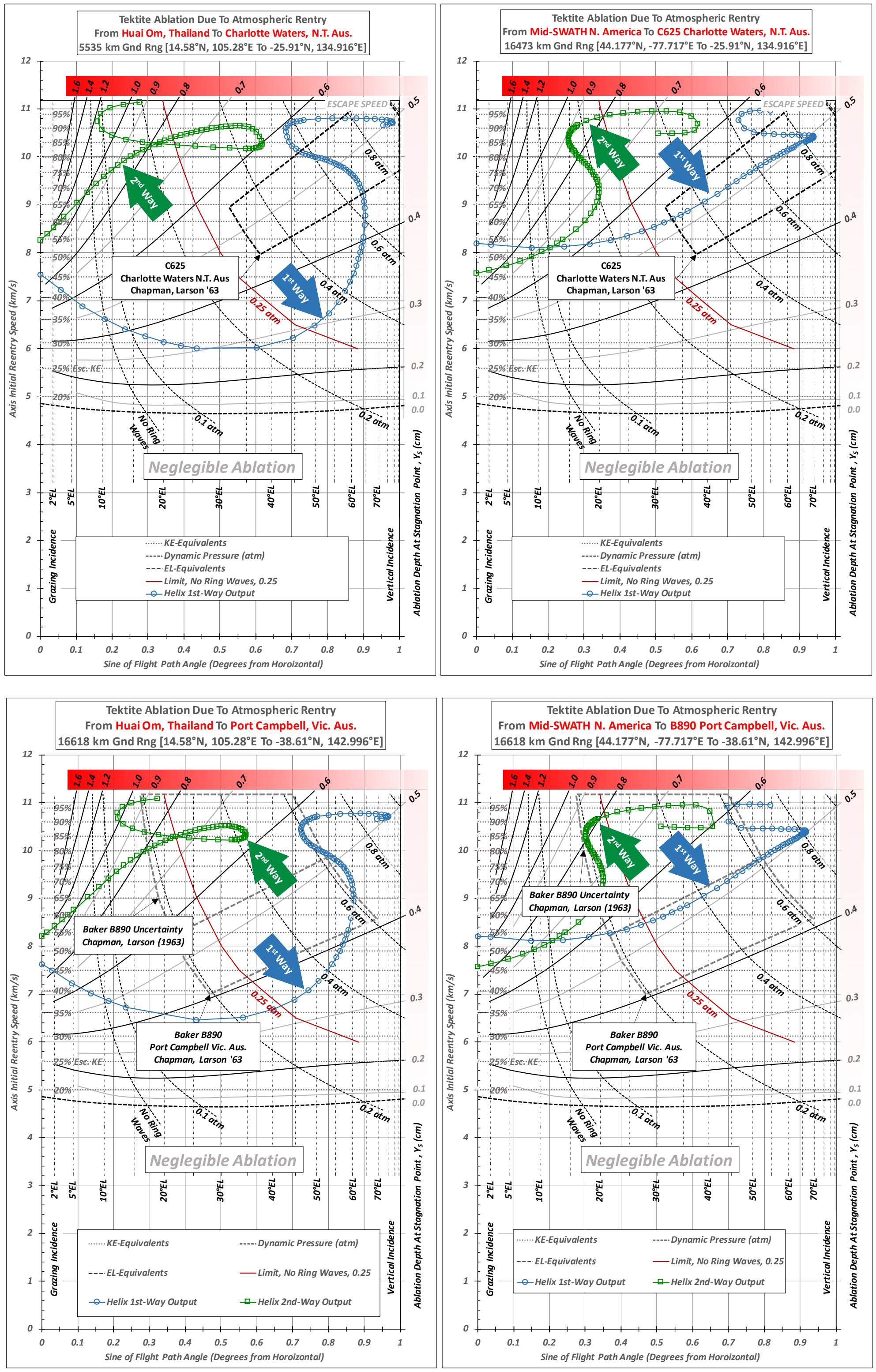

Tektite Ablation Due To Atmospheric Rentry
From Huai Om, Thailand To Charlotte Waters, N.T. Aus.
5535 km Gnd Rng [14.58°N, 105.28°E To -25.91°N, 134.916°E]
C625
Charlotte Waters N.T. Aus
Chapman, Larson '63
Tektite Ablation Due To Atmospheric Rentry
From Mid-SWATH N. America To C625 Charlotte Waters, N.T. Aus.
16473 km Gnd Rng [44.177°N, -77.717°E To -25.91°N, 134.916°E]
Tektite Ablation Due To Atmospheric Rentry
From Huai Om, Thailand To Port Campbell, Vic. Aus.
16618 km Gnd Rng [14.58°N, 105.28°E To -38.61°N, 142.996°E]
Baker B890 Uncertainty
Chapman, Larson (1963)
Baker B890
Port Campbell Vic. Aus.
Chapman, Larson '63
Tektite Ablation Due To Atmospheric Rentry
From Mid-SWATH N. America To B890 Port Campbell, Vic. Aus.
16618 km Gnd Rng [44.177°N, -77.717°E To -38.61°N, 142.996°E]
ESCAPE SPEED
1st Way
2nd Way
Neglegible Ablation
No Ring Waves
0.25 atm
Grazing Incidence
Vertical Incidence
KE-Equivalents
Dynamic Pressure (atm)
EL-Equivalents
Limit, No Ring Waves, 0.25
Helix 1st-Way Output
Helix 2nd-Way Output
Axis Initial Reentry Speed (km/s)
Ablation Depth At Stagnation Point, Y_S (cm)
Sine of Flight Path Angle (Degrees from Horoizontal)

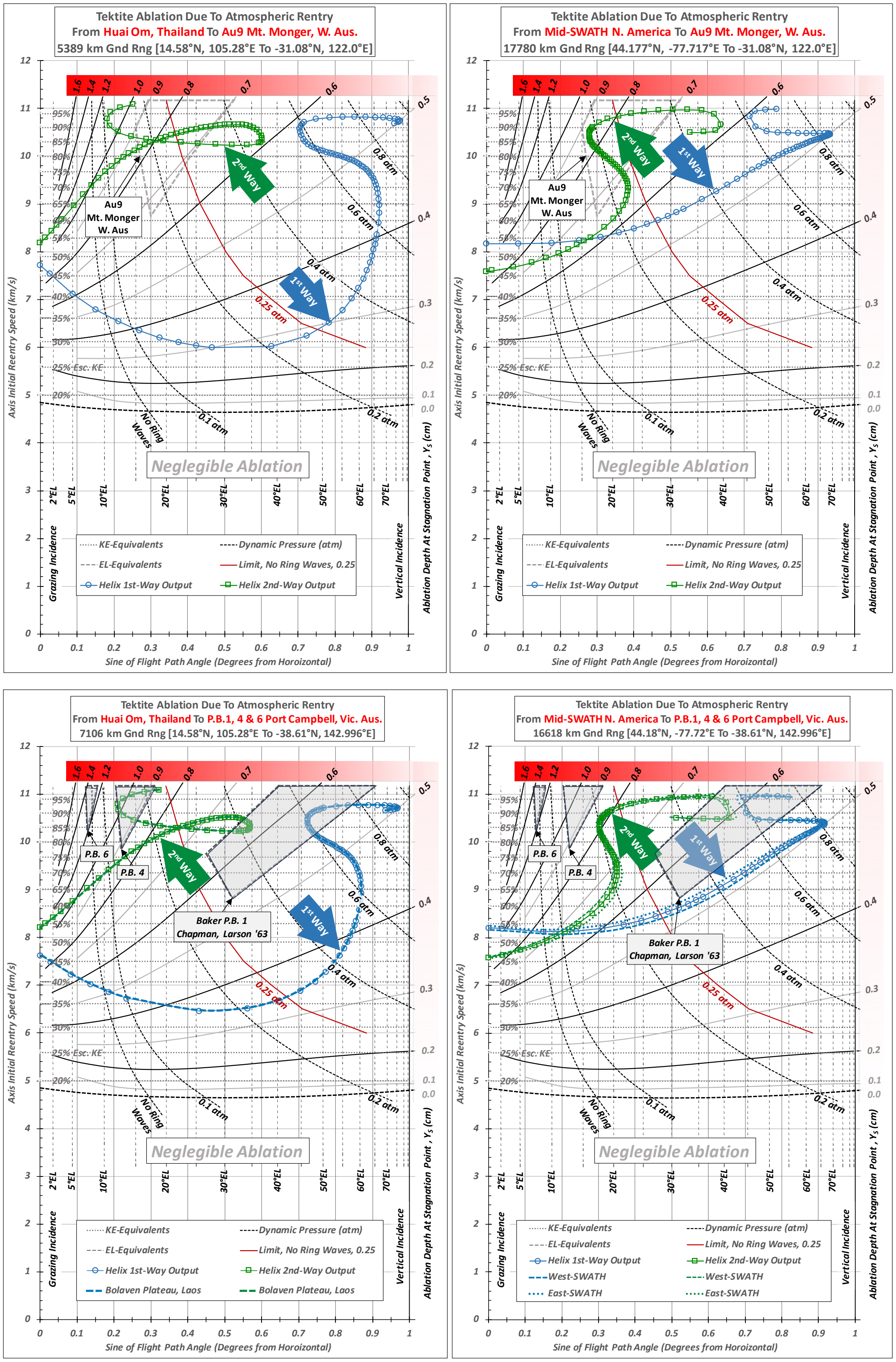

Tektite Ablation Due To Atmospheric Rentry
From Huai Om, Thailand To Au9 Mt. Monger, W. Aus.
5389 km Gnd Rng [14.58°N, 105.28°E To -31.08°N, 122.0°E]
Tektite Ablation Due To Atmospheric Rentry
From Mid-SWATH N. America To Au9 Mt. Monger, W. Aus.
17780 km Gnd Rng [44.177°N, -77.717°E To -31.08°N, 122.0°E]
Tektite Ablation Due To Atmospheric Rentry
From Huai Om, Thailand To P.B.1, 4 & 6 Port Campbell, Vic. Aus.
7106 km Gnd Rng [14.58°N, 105.28°E To -38.61°N, 142.996°E]
Tektite Ablation Due To Atmospheric Rentry
From Mid-SWATH N. America To P.B.1, 4 & 6 Port Campbell, Vic. Aus.
16618 km Gnd Rng [44.18°N, -77.72°E To -38.61°N, 142.996°E]
Au9 Mt. Monger W. Aus
P.B. 6
P.B. 4
Baker P.B. 1 Chapman, Larson '63
1st Way
2nd Way
Neglegible Ablation
No Ring Waves
0.25 atm
Grazing Incidence
Vertical Incidence
Axis Initial Reentry Speed (km/s)
Ablation Depth At Stagnation Point, Y_S (cm)
Sine of Flight Path Angle (Degrees from Horoizontal)
KE-Equivalents
EL-Equivalents
Helix 1st-Way Output
Dynamic Pressure (atm)
Limit, No Ring Waves, 0.25
Helix 2nd-Way Output
Bolaven Plateau, Laos
West-SWATH
East-SWATH

SUPPLEMENT 4:

Lake Huron's Location, Layout and Implications for Indochinite and Other AAT

A diversity of possible launch conditions, suggested launch and early trajectory scenarios, and implications of same, are derived from the geographic layout of contemporary Lake Huron as the modified remnant impact structure of the Australasian tektite (AAT) impact event. The lake has South branch or 'wing' terminating at the St. Clair River, (U.S. Canadian border) and a West 'wing', terminating at the Straits of Mackinac. The entire AAT strewnfield may be populated via suborbital trajectories from the Lake Huron region in only two directions, southerly @~188° AZ and westerly @~278° AZ (both cases +/- a few °), suggesting KE partitioning in those two directions.

The approximate NE-to-SW line of symmetry or 'centerline' may be drawn from the northeast at Beacon Rock in Killarney, Ontario Canada (~45.914° N, ~80.843° W) to the southwest through the center of Charity Island, Au Gres, Michigan (zip code 48703) with coordinates ~44.030° N, ~83. 435° W, in the middle of Saginaw Bay. The island is chosen as a possible central peak of the putative impact structure, convoluted toward the indicated downrange direction by the effects of oblique incidence and volatile overburden per references given in Section 4. Because the impact was presumedly across the Laurentide Ice Sheet and the contemporary layout of the lake represents impact convolution through the thick ice as well as modification since ~789 ka, centerline axis definition is interpretive to some extent.

Using the partitioning concept implied by Lake Huron's planform across the landscape as outlined in Harris, Davias (2017) and Figure 9 of this work, a diversity of launch conditions from the region may be assessed for comparison against observed features of the AAT imprint. Two specific features of the AAT imprint are of interest to explain; 1) the irregular form factors of a large fraction of Indochinite tektites, and 2) the broadly distributed μ-tektite population with approximate concentration peak in the Indochina region per Glass, Koeberl (2006). The latter is often cited in support of an Indochina AAT source by applying proximal ejecta blanket thickness equations ('strategy') to μ-tektite concentration values of ocean core samples, while the former is similarly cited along with lack of observable ablation and the occurrence of Muong Nong-type layered tektites in that region. Both of these concerns are centrally important to the AAT source mystery, and both are explained by careful examination of the suborbital transport paradigm as enhanced by a broad region of surface volatile involvement produced in an oblique impact.

Alvarez (1996) introduces the phrase 'Global Ballistic Sedimentology' while assessing suborbital transport in the K-Pg event paradigm of ~65 Ma, where many details of that event have most likely been erased or altered beyond recognition over that time period. This author labels the ***A***-given-***B*** (inverse) suborbital problem as 'the Chapman problem' in honor of the NASA researcher who largely determined the reentry conditions of ablated AAT in the 1960s. Fortunately, the recent 789 ka AAT event epoch preserves many of the finer details in the form of tektites and their preserved detail, both macro and micro, to bolster the effort of source location. When the source or impact site is missing, we need to assess known ejecta characteristics and their individual locations to narrow possible source regions. Harris (2022) frames the problem as one of KE partitioning audit. Our job as the auditors or *KE partitioning accountants* requires tracking the energy delivered by the projectile, starting with known features of recovered ejecta.

The AAT case is similar to the KPg case because of the colossal scale involved, in terms of both melt mass and its distributed area across the planet more broadly than other tektite event cases. Both seem to indicate melt ejecta propulsion via volatile boosting within the impact fireball or plume. What is missing and perhaps most misleading in the more recent case of the AAT event is any evidence of global conflagration, i.e., burning of the landmass biome, a *critical clue* to the mystery. Hayward et al. (2012) reminds us that the AAT event correlates to global benthic mass extinctions in every ocean basin at every depth, peaking at the time of the tektites. The benthic realm is the most stable biome on the planet, making the AAT case even more important to resolve. Timing detailed in Hayward et al. (2012) shows a ramping up of the extinction rate for 100 ka or more *before* the impact, a red flag to many geologists who discount the possibility of precursor causal relationships per the law of superposition from stratigraphy.

We must picture the Earth in the larger setting of the inner solar system, realizing that a giant comet diverted from the outer solar system to that setting may pass our home planet periodically for an extended period, while decomposing some amount on each pass near our local star. During this period, Earth's local setting in space becomes contaminated with the resulting effluent, changing insolation and delivering debris to our magnetosphere and upper atmosphere. Geology's law of superposition is not valid in this scenario, where an extraterrestrial body (that eventually collides with Earth) may affect our planet for some time before Earth such collision, and this should be no surprise. Traditional or 'Gradualist' geology also rejects the concept of catastrophism, sometimes to the extent that peer review becomes impossible for catastrophic topics or observations, especially within the planetary impact paradigm. Again, we must reframe to the bigger picture. Planetary impact is actually a *gradual process*, in our case as old as the solar system, including planetary formation from accretion through lunar origin and leading all the way to Earth's contemporary status. Looking at individual impact events in the stratigraphic column may lead downward-peering scientists to believe it is a punctuated process. The reality is that we must look both up and down throughout the "vertical column" for a fully formed view of our terrestrial setting.

The current assessment applies 'Informed Imaginative Grey Matter Parallel Processing' (IIGMPP) for the requisite explanations. 'Informed' means based on known scenarios and relationships of the physical sciences, across a wide range of topics in addition to the singular suborbital analysis basis. 'Imaginative' refers to highly associative *cognitive assimilation* (psychology), or the incorporation of new ideas into the known body of knowledge (direct quote from Wikipedia?). This is where reliance on previous laws of impact scaling and ejecta blanket modeling fails in the unique AAT mystery, as shown below. 'Grey matter parallel processing' means using the human brain instead of numerical computational aids, and this is critically important for the cognitive assimilation effort. The AAT imprint has many unique and puzzling features, requiring a large degree of information derived from interdisciplinary topics. Mother nature is an interdisciplinary actor, and Alvarez (1990) reminds us that an interdisciplinary approach involving collaboration and shared language between specialty scientific camps is the only way to solve planetary impact mysteries. We must tear down the fences between camps, not build fences or reinforce existing barriers between different scientific camps. To this effort we may consider the following scenarios…

1) Center-facing or ‘inboard’ tektite ejection trajectories from the South and West ‘wings’ of Lake Huron may intersect upon ascent, with *timing* depending on the inboard AZ angle, launch location along those wings, launch speed and elevation angle. This timing should then be compared to the solidification time for tektites in vacuum to determine if indochinite fragment-forms or other tektite alteration features may have been produced this way. Large volumes of disrupted ice, some of it almost certainly ionized to some extent, would be present in this setting, allowing (relatively) high-density shock waves above traditional exobase height. Electrical charge liberated by shock may seek ground through regions of elevated density, perhaps along ionized silicate ‘trails’ from tektites or proto-tektite mass during this phase. Later ejection of deeper sedimentary strata via Rager et al. (2014) would inject chunks of same into the steam plasma bath to fuse them via high radiant flux of characteristic temperatures in the mid U.V., comparable to the 100% absorption band of Quartz.
2) Steeply vertical jetting from Lake Huron’s south branch with entrained silicates could involve high-shear, turbulent lateral margins to disrupt the melt into μ-tektites. The jet would then expand through rarefaction into exospheric vacuum, spreading out the μ-tektite launch vectors to deliver the observed distribution with peak at the Glass, Koeberl (2006) center roughly over S. E. Asia. Concentric cones of launch angles around a high launch elevation (EL) baseline (Glass-Koeberl (“G-K”) μ-tektite centroid) trajectory will produce fall patterns across Indochina and surrounding regions much like the μ-tektite concentration map of Fig. 10 on p 322 of Glass, Koeberl (2006). The southern-facing branch of Lake

Huron's geographic layout is exactly oriented to produce this effect per Figure 9 of the main manuscript.

Prior abstracts on post-solidus and electromagnetic alteration of Indochinite tektites by this author are provided below as further content supporting electromagnetic (EM) involvement and post-solidus alteration during the Indochinite formative process, of interest to readers who may have never heard of such a concept. It is scarcely mentioned in tektite literature. The Lunar and Planetary Science Conference organizers have been very generous to allow these 'non-standard' observational offerings, which are seemingly important features of the imprint, requiring their own consideration to explain.

Indochinite Suborbital Assessment 54th LPSC 2023 presents some of the conceptual content used in this submission -

iPoster link:

https://lpsc2023.ipostersessions.com/Default.aspx?s=1E-BD-6E-59-86-3A-BD-6F-86-1B-AA-B0-70-5E-BB-53

Harris, T. H. S. (2023) Indochinite Tektite Post-Solidus Alteration LPSC54 abstract no. 1331 p1 of 2 and p 2 of 2 (pdf page copies below) with iPoster link: https://lpsc2023.ipostersessions.com/Default.aspx?s=78-E5-6C-F9-2B-91-B5-FE-2B-8B-5C-CF-8E-A2-17-29 (good 360°Imagery scroll-able videos of altered tektites). This author owns all specimens shown within, and the image acquisition hardware employed to capture the presented content, a key for sharing these wonderful and enigmatic morphologies for the world and especially the scientific community to appreciate. And most of all, thank you LPSC!

Harris, T. H. S. (2023) Indochinite Tektite Post-Solidus Alteration. *54th Lunar and Planetary Science Conference*, abstract no. 1331 p1of 2

INDOCHINITE TEKTITE POST-SOLIDUS ALTERATION. T. H. S. HARRIS[1] [1]GE Astro Space Div., Lockheed Martin, Boeing Helicopter, retired (thsharris1@icloud.com, Brooklyn NY)

Introduction: Formed as early-ejected melt from planetary impacts, tektites are devolatilized and quenched to solid in vacuum as their defining characteristics. The process requires sufficient initial speed for extended loiter above the atmosphere, and cold view factor exposure while in vacuum. Highly ablated tektites are known to be solid upon reentry onset, while lessor ablated fragment-form AAT of S.E. Asia reveal post-fracture visco-plastic strain, evidence of heating and reshaping from a brittle solid state.

The Indochinite subfamily of Australasian tektites (AAT) are often assumed to lie near their source because they appear unablated or only mildly ablated. Tektite ablation during reentry into the standard atmospheric column is a product of speed and sin(θ), where θ is the flight path angle from horizontal per 1960s NASA research [1, 2]. Earth's rotation was typically not considered in the 1960s simplified two-body gravity treatments for tektite suborbital fall patterns as explained in [3, 4], where ablation regime data and suborbital analysis indicate the AAT source region coincident with the N. American Great Lakes.

Irregular and/or tumbling shapes will spread frictional heating over more of their surface area during reentry, reducing or eliminating ablation even at larger fractions of Earth's escape speed or Kinetic Energy (KE), as discussed in [1, 2, 6]. The contorted shapes of Indochinite AAT are typically assumed to be post-depositional imprints, in conflict with the observed feature set for several reasons explained in [6].

Figure 1*. A roughly cylindrical 9 cm long elongate exhibits ridge segments sub-parallel to its long axis in relatively unpitted or 'bald' surface regions. Fragments of hollow spheroidal tektites often contain similar post-solidus visco-plastic imprinting consistent with flow separation during hypervelocity reentry heating.*

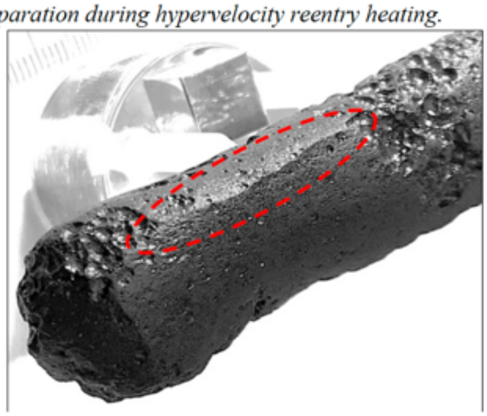

Observed Feature Set: Indochinite 'fragment-form' Australasian tektites indicate post-solidus alteration from externally applied mechanical forces to generate fracture, followed by rapid (fractional second) heat deposition across bulk mass (body-applied heating), often observable on hollow spheroid fragment and other splashform shapes. Figure 1 presents aerodynamic shaping on a cylindrical 'elongate' tektite.

Convoluted imprint. Tektite alteration via explosive heat deposition and subsequent visco-plastic momentum imprinting via high-voltage arcing through the tektite's plasma sheath as suggested in [6] is problematic. This requires a high-energy reservoir near the tektite descent corridor over the S.E. Asia region, probably *many hours after* the causal event. It does explain the pristine heat glaze on may indochinite fragment-forms, where no steady state hypervelocity flow field would establish around a rapidly tumbling irregular shape and the brief heating pulse of several thousand degrees would distribute across the full tektite surface to minimize melting.

Descent-phase disruption of indochinite AAT before or during reentry may correspond with the rapid heat and humidity pulse after the blast, as required to laterize the top of impact clastic unit 2 at Huai Om Thailand where tektite fragments are found, per [7]. Before active dissection could take effect, the tropical landscape with tektite topping at Huai Om was covered with meters of fining-upward angular quartz sand, the rapid regional laterization engine perhaps the sand weight atop a highly compressed, wet atmosphere?

Post-fracture visco-plastic shapes. Common indochinite AAT morphometric trends include fragments of hollow spheroids with out-of-plane visco-plastic deflection on apparent fracture planes. Sometimes this manifests as raised rims at a pock in the spheroidal shell per Fig. 2A, or more commonly as raised rims around concave bubble margins per Figure 2B, 2C/D. Figure 2B & 2C/D could be evidence of a warm core upon fracture of the cooler outer spheroidal tektite volume, while the unique feature of Figure 2A lacks such explanation. All specimens are shown with a 1 cm scale cube for reference.

Reentry heating at tektite speeds lasts for a few tens of seconds, largely insufficient for bulk heating of the overall tektite mass to produce body-heated visco-plastic effects. Figures 3 and 4 may result from stress-generated cracks and differential erosion for striae relief, but this is not always the case per [6]. Radiant flux of high-voltage arcing could produce these effects

Harris, T. H. S. (2023) Indochinite Tektite Post-Solidus Alteration. *54th Lunar and Planetary Science Conference*, abstract no. 1331 p2 of 2

on cold glass in *millisecond* timescales, along with second-timescale chill upon arc termination.

Figure 2*. Evidence from N. E. Thailand of post-fracture visco-plastic deformation requiring tektite re-heating. A: Shell segment w/ through-wall raised-rim pock at scale cube. B, C and D are fragments of hollow spheroids, C and D are same specimen where both sub-planar surfaces have raised bubble rim margins.*

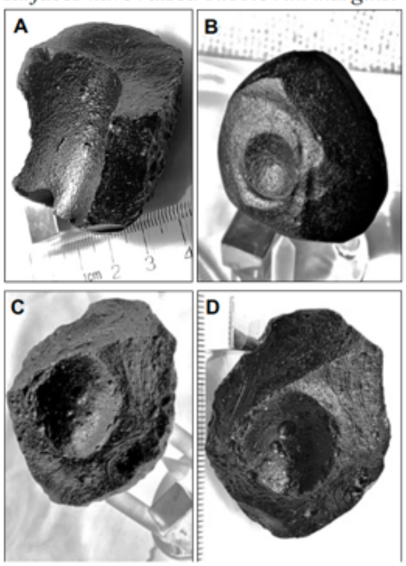

Figure 3*. A: Tektite shell fragment has melt 'tongue' extending from concave surface across part of the wall thickness, with a score across the root of the tongue. B: Closeup of fragment wall w/ scored tongue shows a sub-parallel striae bundle emanating from the score mark. Score mark excavation and sub-parallel striae are consistent with high-voltage arcing and magnetic field.*

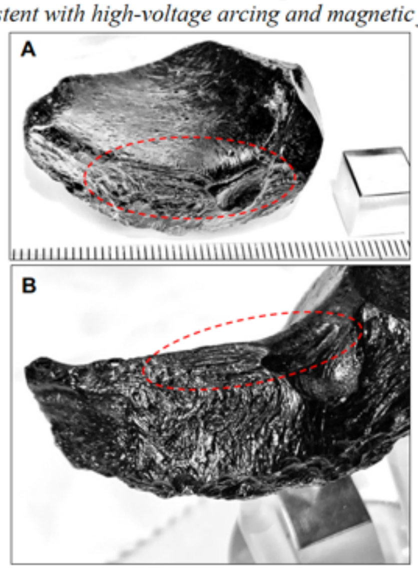

Figure 4*. A hollow tektite fragment exhibits a gouge along its wall beneath the concave surface in image A. The gouge, in a form often assumed to be post-depositional cracking eroded to width over time, travels from the convex, deeply pitted outer surface across the wall thickness and then parallel to the concave surface margin, lower to upper image B. Beneath the gouge on another apparent fracture surface in image C is a concentrated, closed-loop cluster of deep-relief striae consistent with high-voltage arcing and magnetic field.*

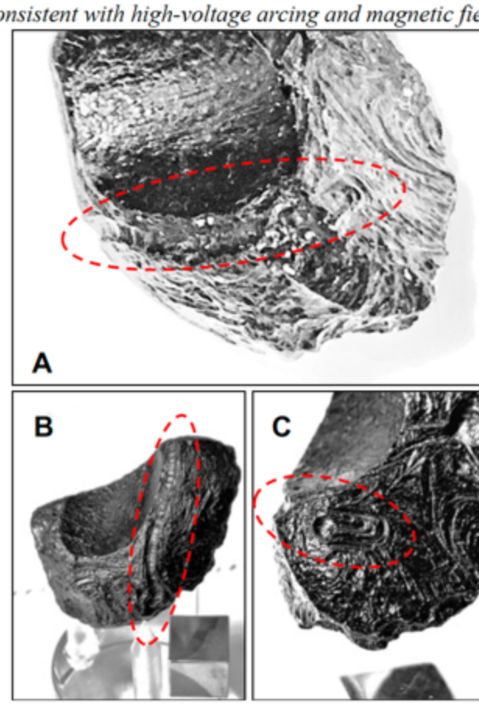

Summary: Simple or symmetric ablation on asymmetric Indochina tektites ('fragment-forms') should not be expected, while lack thereof should not be used for assumptions of Australasian tektite reentry speed. The feature-set convolution is complex. An energy reservoir must have existed over S.E. Asia along the tektite descent corridor in order to fragment this AAT subgroup *and* laterize the regional tektite-bearing surface *within hours* before uneroded burial, suggesting high-potential E-fields and full-height disruption of the atmospheric column from exosphere to surface.

Acknowledgments: This work was self-funded

References: [1] Adams, Huffaker (1962) *NASA Technical Report R-149*. [2] Chapman, Larson, Anderson (1963) *NASA Technical Report R-134*. [3] Harris (2021) *LPSC 52,* Abstract #1008. [4] Harris 2022 *GSA Books 553* Ch 23. [5] Sepri, Chen, O'Keefe (1981) *JGR* vol. 86, No. B6, 5103-5111. [6] Harris (2021) *LPSC 52,* Abstract #1009. [7] Tada et al. (2022) *Meteoritics & Planet. Sci.* 57, Nr 10, 1879-1901.

Harris, T. H. S. (2021) Electromagnetic Indications of Australasian Tektite Morphology.

52nd Lunar and Planetary Science Conference, abstract no. 1009, p 1 of 2

52nd Lunar and Planetary Science Conference 2021 (LPI Contrib. No. 2548) 1009.pdf

ELECTROMAGNETIC INDICATIONS OF AUSTRALASIAN TEKTITE MORPHOLOGY.

T.H.S. HARRIS, GE Astro Space Div., Lockheed Martin, Boeing Helicopter, retired (thsharris1@icloud.com)

Introduction: Indochinite Australasian tektites (AAT) display contorted unit morphology consistent with electric charge saturation, arc-induced heating during magnetic confinement, and magnetic flux expansion with rapid cooling. Common surface textures are consistent with post-solidus flash heating and coincident electromagnetic (EM) field imprinting. Common co-expression of these Indochinite 'fragment-form' tektite features is consistent with disruption by high voltage (HV) arcing in vacuum, requiring explanation.

Fragment-Form Evidence: Two ~3cm-scale spheroid fragment-forms show apparent HV arcing imprints.

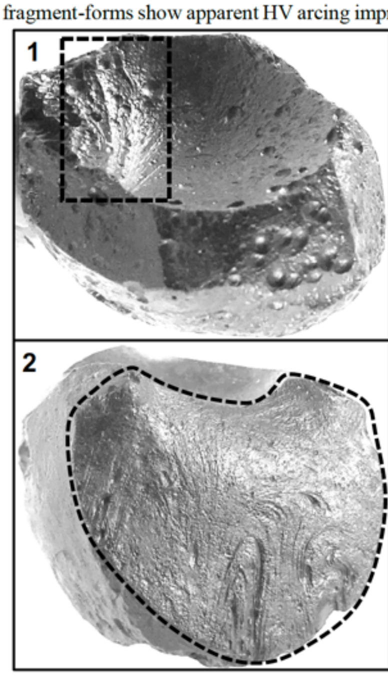

Top (1): arcing melt track across left portion of the concave surface with radiating filaments. *Bottom* (2): apparent surface layer EM field line striae imprinted by HV arcing. Both imply initially solid condition.

A proposed sequence fits the observations, with arcing timescales explaining rapid thermal cycling. Post-deposition differential etch is inconsistent with AAT splash form melt homogeneity. The indicated KE scale is similar to that of uniquely high test-derived and triple-verified AAT reentry speeds of 80% or more of Earth escape speed per NASA and Chapman et al. (1964) [1] as well as the uniquely broad AAT strewn coverage. These multiple indications of 'extinction-level' KE scale are also considered for further AAT event insight.

Lab Evidence Extended: Kurosawa et al. (2012, 2015) [2, 3] explain *the role of the electron* in shock partitioning. *Elevated H_2O* is suggested per Watt et al. (2011) [4]. H_2O ionization and non-equilibrium shock processes discussed by Skryl et al. (2007) and Khantuleva (2003) [5,6] respectively, explain induced electrical current from strong shock, as correlation-length reduces to the order of H_2O molecular dimension. An inductive-capacitive 'LC' circuit model provides an approximation; with extended period $\tau \propto \sqrt{L * C}$, planetary-scale inductive and capacitive reactance are indicated by τ on the order of tektite melt cooling time.

EM Alteration Sequence: The setting is H_2O component plasma and high induced electric field from shocked ice. Left column (pg. 2) images show radiant flux stripping silicate ions (1) which stream away as a conductive path in the surrounding high potential electric field, leading to high-voltage arcing through the tektite (2). Arc-induced heating adds ions, lowering conductive impedance, increasing current and heating, and fracturing the solid tektite shell (3). Current-induced magnetic field compresses the body-charged tektite (4), trapping fragments during energetic plasma venting erosion (5). Right column shows a compressed discoid fragment (1 & 2) with bulged plastic core A, plasma-eroded facets B and dissimilar exterior and fracture surfaces C. Hollow spheroid fragment (3) shows radial striae on surface A. Truncated spheroid (4) shows raised-rim deposition point A, plasma erosion facet B, fracture plane C and exterior pitting D. Frames (5) and (6) show 'extruded' hollow tektite fragments, with arrow showing extension direction. Scale cube is 1 cm.

Conclusions: EM involvement in post-solidus AAT disruption and thermal alteration is indicated by indochinite fragment-form specimens. Convex surface pitting and pock marks are consistent with post-solidus particle or spatter bombardment during thermal cycling in vacuum. Extensive target mass H_2O ice is indicated, perhaps from large projectile or expanded oblique impact footprint and associated multiple in-track hotspots.

References: [1] Chapman et al. (1964) *Gochimica et Cosmochimica Acta* Vol. 28 p. 841-880. [2] Kurosawa et al. (2012) *JGR*, 117 E04007. [3] Kurosawa et al. (2015) *JGR Planets* [4] Watt et al. (2011) *M&PS*, 46, Nr 7, 1025-1032 [5] Skryl et al (2007) *Physical Review B* 76, 064107 [6] T.A. Khantuleva (2003) in *High-Pressure Shock compression of Solids VI*, Springer.

… and…

Harris, T. H. S. (2021) Electromagnetic Indications of Australasian Tektite Morphology

52nd Lunar and Planetary Science Conference abstract no. 1009, p 2 of 2

52nd Lunar and Planetary Science Conference 2021 (LPI Contrib. No. 2548) **1009.pdf**